NOVA SCHOOL OF SCIENCE & TECHNOLOGY

DEPARTMENT OF PHYSICS

SARA RAQUEL FERREIRA MENDES

BSc in Biomedical Engineering

ELECTRODE FABRICATION THROUGH ADDITIVE MANUFACTURING AND THERMOPLASTIC NANOCOMPOSITES

MASTER IN BIOMEDICAL ENGINEERING

NOVA University Lisbon

September, 2024

NOVA SCHOOL OF
SCIENCE & TECHNOLOGY

DEPARTMENT OF
PHYSICS

ELECTRODE FABRICATION THROUGH ADDITIVE MANUFACTURING AND THERMOPLASTIC NANOCOMPOSITES

SARA RAQUEL FERREIRA MENDES

BSc in Biomedical Engineering

Adviser: Henrique Vazão de Almeida
Assistant Researcher, NOVA University Lisbon

Co-adviser: João Oliveira
Full Professor, NOVA University Lisbon

MASTER IN BIOMEDICAL ENGINEERING

NOVA University Lisbon
September, 2024

Electrode Fabrication Through Additive Manufacturing and Thermoplastic Nanocomposites

This document was created with the (pdf/Xe/Lua)LaTeX processor and the NOVAthesis template (v7.1.29) [45].

Acknowledgements

I want to start by expressing gratitude to my adviser Professor Henrique, and my co-adviser Professor João, for their continuous support during these months. This dissertation would not be possible without their encouragement, creativity and enthusiasm.

I am very thankful to Maria, Rui and Tomás for their incredible patience in answering all my questions, their availability to help whenever needed, and their innovative ideas that enriched this project.

I also like to thank CENIMAT | i3N and its team for welcoming me and supporting this journey, as well as NOVA School of Science and Technology for the 5 years that led to this work.

To my lab partner Margarida a huge thank you, together we made it, even with doubts and setbacks, without you this work would not be possible.

To all my friends who made this journey unforgettable, who made the bad days happier, with who I can always share a laugh and who always believe in me thank you.

L, M, F and F wherever you are, I will never forget what you all have done for me. Thank you for being by my side throughout all of this journey.

To my special person, there are not enough words to describe how grateful I am for having you by my side. All the hours listening to me and my problems and working together to find solutions, I can not thanking you enough. You are my sun, always making my days brighter.

Finally, to my parents, sister and aunt, thank you for making me believe that nothing is impossible, for pushing me to be my best and for always believing in me and my dreams, without you this work would not be possible. You all made me a better person, who never gives up on her dreams no matter how hard to achieve they are. Thank you.

Abstract

In the present day, additive manufacturing, also known as 3D printing, is becoming a more common and relevant technique. Additive manufacturing provides an easy and cost-effective way to fabricate devices that can be easily personalised, by changing the design to enhance performance and/or adapt to the dimension of the patient's body. These characteristics make this method quite appealing to the healthcare world that needs to provide simple and practical solutions for the expanding demand for care.

Nowadays there is an increased concern about patient comfort during exams and medical procedures. One of the devices that can improve in this area are electrodes. Electrodes work as an intermediate between the biosignals and the biosensor circuits. Surface electrodes are a non-invasive technique for analyzing electrophysiological signals. These devices are an essential tool for performing multiple exams such as Electromyography (EMG), Electrocardiogram (ECG) and Electroencephalogram (EEG). There is also a demand for electrodes capable of analysing muscle groups instead of just one muscle.

In the last few years there have been more and more studies to utilize additive manufacturing to fabricate electrodes. These studies have successfully created electrodes that can be replicated using low-cost materials (e.g. thermoplastics) that are commonly found in the market. Besides that, 3D printing is especially appealing for wearable devices since it allows the personalization of care and allows easy adaptability of the design to the patient's needs and features.

In this dissertation it is proposed a prototype device of an electrode capable of capture electromyography signals of the biceps and triceps simultaneously, that allows the evaluation of the muscle activity.

The research work described in this dissertation was carried out in accordance with the norms established in the ethics code of Universidade Nova de Lisboa. The work described and the material presented in this dissertation, with the exceptions clearly indicated, constitute original work carried out by the author.

Keywords: Additive Manufacturing, Conformable electrode, Electromyography, Muscle Activity, Wearable Device

Resumo

Nos dias de hoje, a fabricação aditiva, também conhecida como impressão 3D, tem-se tornado uma técnica mais relevante e comum. A fabricação aditiva potencia uma forma simples e de baixo custo, de fabricar dispositivos que podem ser facilmente personalizáveis, mudando o design para melhorar a performance e/ou para permitir uma melhor adaptação ao corpo do paciente. Estas características fazem este método bastante interessante para o mundo da saúde que precisa de soluções simples e práticas para a crescente demanda de cuidados.

Atualmente há uma crescente preocupação com o conforto dos pacientes durante exames e procedimentos médicos. Um dos dispositivos que pode melhorar nesta área são os elétrodos. Os elétrodos funcionam como intermediários entre os sinais fisiológicos e os circuitos dos biossesnores. Os életrodos de superfície são uma forma não invasiva de analisar sinais eletrofisiológicos. Estes dispositivos são utilizados para realizar diversos exames tais como eletromiografia, ecocardiograma e electroencefalograma. Para além disso, há também uma grande procura de métodos para analisar grupos de músculos em vez de apenas um músculo de cada vez.

Nos últimos anos têm havido cada vez mais estudos em que a impressão 3D é utilizada para fabricar biossensores, e têm sido bastante bem sucedidos em criar dispositivos que podem ser facilmente replicados usando materiais de baixo custo, como por exemplo, termoplásticos que são facéis de obter no mercado.

Nesta dissertação é proposto um protótipo de um elétrodo capaz de avaliar a atividade muscular simultaneamente do bícep e do trícep através da captação sinais de eletromiografia. O trabalho de investigação descrito nesta dissertação foi realizado de acordo com as normas estabelecidas no código de ética da Universidade Nova de Lisboa. O trabalho descrito e o material apresentado nesta dissertação, com as exceções claramente indicadas, constituem trabalho original realizado pela autora.

Palavras-chave: Atividade Muscular, Dispositivo "Wearable", Elétrodo Conformável, Eletromiografia, Fabricação Aditiva

Contents

List of Figures

List of Tables

Acronyms

ABS Acrylonitrile Butadiene Styrene *(pp. 10, 12)*
Ag/AgCl Silver Chloride Electrode *(pp. 1, 6, 25, 30, 34, 39)*
ALS Amyotrophic Lateral Sclerosis *(pp. 2, 4)*

ECG Electrocardiogram *(pp. iii, 1, 6, 10, 11)*
EEG Electroencephalogram *(pp. iii, 1, 6)*
EMG Electromyography *(pp. iii, v, 1–7, 9–11, 13, 27, 30, 33, 34, 37–40)*

FDM Fused Deposition Modelling *(p. 13)*

LIG Laser-Induced Graphene *(pp. 1, 7, 9, 22, 26)*

PLA Polylactic Acid *(pp. 1, 10, 12, 13)*

SD Standard Deviation *(p. 28)*
SR Sheet Resistance *(p. 28)*

TPU Thermoplastic Polyurethane *(pp. 1, 2, 9–13, 16, 20–29, 38, 39)*

1

Introduction

1.1 Motivation

Nowadays, electrodes are widely used in the medical field and have multiple proposes. These devices have a conductive material that makes contacts with the skin and establishes the connection between the patient and the biosensor circuit. Besides, allows the reading of electrophysiological signals in a non-invasive way, when combined with biosensors, electrodes serve as a transducer for EMG [87], ECG [28], EEG [29] and other electrophysiological signals monitoring. Besides, electrodes are also used to send electrical current into the body of the patient, for example as defibrillator [46]. Another example is neurostimulation [30].

There are multiple techniques for developing electrodes and several materials can be used as electrodes. Depending on their final application, while some methods are simple and affordable, such as Laser-Induced Graphene (LIG) electrodes [68] made by laser engraving on paper, which presents a low cost, and it is possible to change the LIG pattern easily, others are more complex such as commercial electrodes of Silver Chloride Electrode (Ag/AgCl), that are more commonly used. [11].

One way to fabricate electrodes is by using additive manufacturing. This method, also known as three-dimensional (3D) printing involves the design of the device using CAD software like *SolidWorks* [1] or *Fusion 360* [2], allowing a profound level of personalization for the device being designed. This feature is particularly convenient for medical applications, especially for wearable devices, since it allows to adapt the device to the body of each patient [64]. For this process many materials can be used, such as biomaterials, metals, ceramics, or polymers [7]. However, thermoplastics are one of the cheapest, easiest to manipulate and most widely used materials [49], specially Polylactic Acid (PLA) and Thermoplastic Polyurethane (TPU).

[1] Solid Works - https://www.solidworks.com/
[2] Fusion 360 -https://www.autodesk.pt/products/fusion-360/overview

1.2 Proposal

Having all the above information in mind, in this dissertation it is proposed a self-standing electrode for EMG monitoring. The electrodes will be fabricated through additive manufacturing using two different materials. The support material will be polyurethane whereas the conductive part of the electrodes will be printed using a conductive filament. As support material, we will use TPU, a flexible thermoplastic. The proposed methodology allows the production of fully 3D printed electrodes without adding extra steps to the process such as patterning.

The final prototype will allow to analyze the activity of upper arm muscles, its activation levels and maximum amplitude reach. EMG is a diagnostic tool that allows the assessment of the patient's motor skills as well as the muscle response to different stimuli [10].

In this dissertation, it is aim to develop a new form to evaluate the damage and monitoring the progression of muscle degenerative diseases, such as Amyotrophic Lateral Sclerosis (ALS), muscle dystrophy and spinal muscle atrophy. Using a wearable device, made especially for each patient according to their unique diagnosis and characteristics, in a personalized, comfortable and efficient approach, by using recyclable materials and creating a reusable product. The prototype could be used to monitor and diagnose degenerative diseases that affect motor skills, as it can monitor the muscular activity of different muscle groups, making the process more comfortable and practical for both patients and healthcare workers.

1.3 Document Structure

In the next chapters it will be discussed the following topics:

- **Fundamental concepts:** The theoretical concepts needed in order to understand the work developed during this work, such as what is electromyography, muscle activity, degenerative diseases and additive manufacturing;

- **State of the art:** The state of the art of EMG electrodes and 3D printed electrodes;

- **Materials and Methods:** In this chapter it will be explored the materials and methods used to develop not only the final propotype but also different designs tested thorughout the thesis to obtain self-adhesive electrodes. The different designs tested will be presented as well as the protocols applied to achieve a conductive surface;

- **Results and Discussion:** The results regarding the characterization of the constituent materials of the produced electrodes, namely the Raman spectroscopy studies will be presented in order to determine the materials present in the filaments used. Also listed will be the studies of the electrical properties of these materials and the electrodes, performed using impedance assessments and sheet resistance verification;

- **Conclusion and Future Work:** we will present a summary of the work done, by looking at all the results obtained through the impedance study, the sheet resistance, the raman spectroscopy and the EMG aquisition. The future work prospects will also be discuss.

2

Fundamental Concepts

To effectively present this work, it's essential to introduce and clarify fundamental concepts that will aid in understanding the proposed ideas, as well as the production process and the functioning of the electrodes. This chapter is divided into six sections, starting with the importance of EMG monitoring in degenerative diseases patients, followed by a detailed explanation of electromyography and electrodes, their fabrication and its challenges. Finally, additive manufacturing methods will be stated. This chapter will be finished by analyzing electrically conductive materials.

2.1 Muscles, their diseases and movements

2.1.1 Muscle Degenerative Diseases

Degenerative diseases can cause muscle degeneration which often leads to weakness or even total disability of the muscles impacted by these disorders [74]. These dystrophies do not have a specific age to manifest, however muscle degenerative diseases diagnosed during childhood often lead to severe problems later in life such as loss of cardiac and respiratory functions. For adults, it is possible that the diagnose can be translated in a slow progression disease that may lead to minor debility and/or the inability to create new muscular tissue [51].

One of the most fatal diseases that affect the muscles and motor system is Amyotrophic Lateral Sclerosis ALS [39]. This disorder is idiopathic and fatal with the first symptoms being fatigue and difficulty in doing any type of physical exercise, which eventually will evolve to a point that will cause malnutrition and respiratory failure, since the deglutition muscles and thorax muscles can become too weak to perform these tasks [34]. To diagnose and monitor the evolution of the disease, EMG is a valuable tool. The most traditional method is intrauscular EMG of the tongue, which is being replaced by the surface EMG of the trapezius muscles [71]. Using artificial intelligence and EMG, it is possible to make the diagnose only by analyzing the movement of the biceps brachii muscles [66].

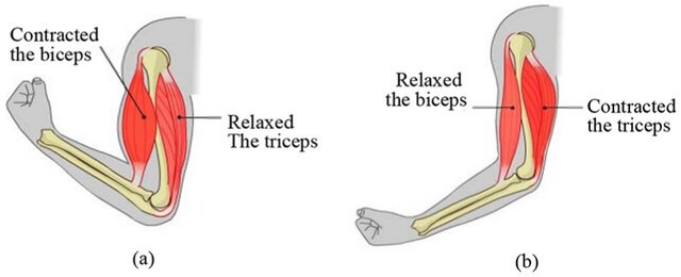

Figure 2.1: Activation of the Bicep Brachii and Triceps muscles. Source: [86]

2.1.2 Muscles Movements

The upper arm has four muscles, three on the anterior part of the arm: biceps brachii, brachialis and coracobrachialis, and one in the posterior part of the arm: triceps brachii [4]. For this dissertation, the most relevant ones will be the biceps brachii and the triceps brachii, which will be explained in more detail ahead. These two muscles are placed in opposite places of the arm and are easily accessible, which makes the process of developing an electrode to measure both muscle's activity simpler.

The biceps brachii performs the movement of flexion of the elbow and the supination of the forearm [37]. On the other hand, the tricep brachii is responsible for the extension of the elbow [3]. These movements are essential to everyday life tasks, such as using a fork, brushing teeth or to reach an object from a bookshelf. It is possible to see these details by looking at Figure 2.1. The movement performed by these muscles is complementary to each other: when the biceps has its peak of activity, triceps activity lower, and vice-versa.

2.2 Electromyography

To evaluate muscle activity, it is needed an EMG sensor and electrodes. EMG measures the electrical signal produced by the muscles when they are activated, as shown in Figure 2.2. The sensor will detect the motor unit potential that is generated by the muscle fibers during the muscle activity. According to the muscle sliding theory, the contraction of the muscles occurs due to the sliding of two muscle filaments: myosin and actin[26], present in the sarcomere, the unit cell of the muscle. When the distance between the myosin and the actin decreases, the actin filaments slide to the myosin filaments, reducing the length of the sarcomere and leading to muscle contraction [70]. Usually, these measurements are made by electrodes placed on the surface of the skin (Surface EMG) or through a needle inserted in the muscle (Intramuscular EMG) [58].

The human body moves due to the contraction and relaxation of muscle fibers. All of this is controlled by the brain either consciously, when we have a voluntary movement, or unconsciously, when we react to a stimuli and have an involuntary movement [50].

Electrodes can be used to detect anomalies and activation levels [25]. EMG is a valuable tool as it can be used to study different conditions, namely muscle fatigue [55], nerve

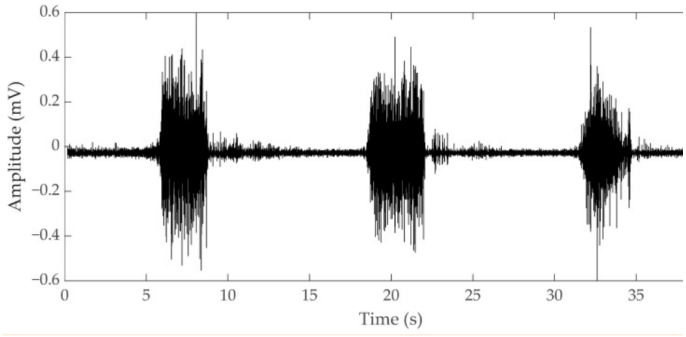

Figure 2.2: EMG Signal during contraction and relaxation of the bicep, acquired using commercial Ag/AgCl electrodes. Source: [55]

damage or muscular problems When a patient cannot perform any type of movement, EMG sensors can be very helpful, since they can determine if the lack of movement is due to nerve or muscle damage. If the problem is in the muscle, the sensor is still able to measure an electrical signal, otherwise, if the damage is in the nervous system, the sensor will not detect any signal. All these measurements can be performed non-invasively, by placing electrodes on the patient's skin, increasing the comfort of the subject.

2.3 Electrodes

In this section, it will be discussed what are conventional electrodes, how they work and some methods for their fabrication. Also, it will be explored the challenges and problems that the most used commercial electrodes face nowadays.

2.3.1 Electrodes and their Fabrication

The human body produces electric signals that can be measured with multiple techniques. The human body produces electrical signals, called electrophysiological signals: in the brain, the synapses, can be measured by anEEG [8], furthermore, ECG, is an exam that records heart electrical signals [62]. The muscle's electrical activity can be analysed by EMG.

Electrodes capture these electrophysiological signals. They work as a transducer and are composed by a conductor material and a support material [80].

In our days, the most commonly used electrode is the Ag/AgCl, which, like the name references, is made with silver and silver chloride as conductive materials. The remaining portion of the electrode is made of disposable materials making these devices non-reusable. Besides, these electrodes also use electrolyte gel to enhance their performance.

Electrodes can be fabricated using multiple methods, ranging from moulding to additive manufacturing. Each process presents different characteristics with different advantages. It will be explained in detail three of these processes, starting with one of the most commonly used, followed by two of the most recent and innovative process:

- Screen printing is a method to fabricated electrodes. This technique consists in the depositing of a material on a plane surface, like glass, and pressing it through the screen, creating the electrode [1]. This is called the thick-film methodology. There is also the thin-film method, where the methodology is similar to the thick film , but the mesh of the screen has smaller dimensions. This procedure makes the final product more flexible, so it is widely used for wearable devices that require a better conformability with the skin [16].

- Laser-Induced Graphene (LIG) can be made by photothermal conversion of a paper substrate using a CO2 laser. The laser creates graphene structures that are conductive, this happens due to rearranges in the carbon hybridization [79], generating a functional electrode [59]. This method can be applied to other materials, such as cork [69], or can be water peel transferred to different substrates that would not react or could not be used in the laser [60].

- Additive manufacturing, in the last few years, has also become a popular method to produce electrodes. Using a filament of conductive material, this methodology allows a deeper personalization, has a lower cost when compared with other methods, and is overall a simpler way to fabricate these devices [44, 84].

2.3.2 Conventional Electrodes Challenges

The commercial electrodes used nowadays present certain limitations. Firstly, all use some type of adhesive to adhere to the skin. This can be painful for patients when the electrode is removed. Moreover, the adhesive can cause allergies for patients with sensitive skin. Secondly, these devices have a gel to lower the impedance between the electrode and the skin which can also cause allergic reactions, particularly if used for long periods of time [72]. Furthermore, the conformability of these electrodes with the skin is limited, especially when the exam requires the patient to perform any type of movement, which is very common in EMG [83]. Finally, the majority of the conventional Ag/AgCl electrodes are not reusable or recyclable, which translates into high waste and costs in terms of production and materials.

2.4 Additive Manufacturing

Additive manufacturing is a technology that is evolving every day, since it is a cost-effective method, simple to use and very versatile, allowing the expansion of its applications in multiple fields. The growing tendency to personalize medical care has increased the search for techniques to produce diagnostic and monitoring systems adapted to each patient. In this regard, the additive manufacturing technique can become a valuable tool, as it allows the size of the printed pieces to be easily adapted to the user. Additive manufacturing (also known as 3D printing) can be divided into three categories of processes: extrusion

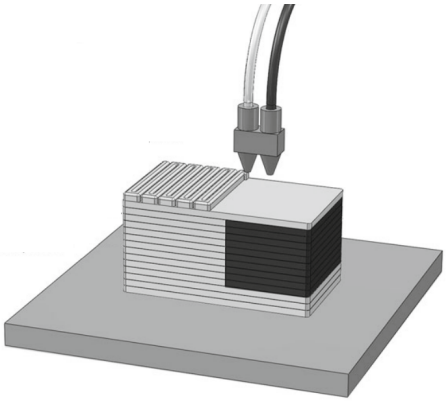

Figure 2.3: Additive manufacturing through extrusion Deposition. Source: [21]

deposition, powder binding and photopolymerization [63]. In this project, it will be used Extrusion Deposition, the most common process, since it is simple, cost-effective and has easy-to-use materials. These materials are usually thermoplastics, composites, or metals.

This method is based on the deposition of multiple layers of the material, as shown in Figures 2.3 and 2.4, through a layer-by-layer deposition [6]. The newly formed layer hardens quickly in the air, serving as a base for the following layer [63]. There are multiple processes of extrusion deposition, the most popular one being filament-based, where the printer needs to be fed with a material in filament form. Using a filament can have some disadvantages, such as small variations in the diameter of the filament, which can lead to blocking, compromising the final result of the print.

One alternative to Extrusion Deposition is a screw extrusion-based methodology. Instead of a filament, it uses granulate material, which is heated and then melted. After that, it is led to the nozzle by the screw. This method has some advantages: it does not need extra processing of the filament beforehand, there is a larger range of materials that can be used and has less degradation derived from high temperatures, since the material is melted more uniformly [76]. Generally speaking, thermoplastics are the chosen option for this type of additive manufacturing. Thermoplastics are polymers that above a certain temperature, called the molten state, become soft or liquid. The process is reversible, which means that when the temperature drops, the material returns to its natural solid state [63].

The properties of the final piece will be influenced by several factors such as: the additive manufacturing technique chosen for its production, the print speed, the temperature of the extrusion and printing bed, the type of filament used and lastly the printer itself [5].

2.5 Electrodes: constituints and materials

In order to read the electrical biosignal, it is needed to have a material that conducts electricity to use as an electrode [38]. To achieve this, multiple materials can be used, such as graphene oxide [35], graphite [67], metal oxides [13], and more recently, MXenes [85] .

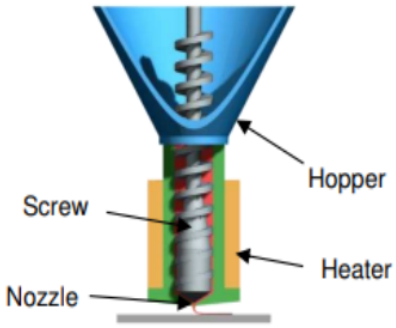

Figure 2.4: Additive Manufacturing through screw extrusion Deposition. Source: [76]

Carbon-based materials, like graphene oxide and graphite, not only have a high electrical conductivity but also a high thermal conductivity. Graphite is one of the most used carbon-based materials since it is low cost and is easily found with a high purity [12].

One way to create carbon-based materials is through laser engraving. Laser patterning uses a laser beam to generate carbonization of the material, making the surface conductive in a simple and efficient way [14]. For substrates like paper, LIG has been used successfully to make electrodes [59] for electrophysiological signals. The high temperatures caused by the laser rearrange the chemical bonds between atoms, making them rearrange and forming the graphene[78].

Another simple option to have a conductive layer is using a conductive filament during the 3D printing. These filaments are usually carbon-based and provide an efficient way to use additive manufacturing to create functional devices [33]. This method allows to have a functional electrode with a support material, using just one printer, as long as it has two extruders. Besides, it is possible to make conductive layers between the support material, allowing tunning the electrode area and its conductivity.

2.6 Summary

In this dissertation we propose the fabrication of electrodes for surface EMG, for measurements in the upper arm muscles biceps and triceps, using additive manufacturing. Using a flexible thermoplastic material (TPU) as base filament for the prototype, it is possible to develop electrodes more flexible and conformable with the skin of each patient, without using any type of adhesive, avoiding skin irritations and allergies. Then, by using 3D printing for fabrication, its possible the personalization for each patient, according to the needs and physiological characteristics of the individual. Furthermore, the final product will be reusable and recyclable. Additionally, the presented production process is time- and cost-effective, which jointly with the easy customization points to the promising future of the developed electrode as a fundamental tool for EMG monitoring.

3

State of the Art

In this chapter, it will be discussed the state of the art of electrodes for EMG namely self-adhesive and self-standing electrodes. It will also be presented a variety of devices manufactured with distinct materials and methods, in order to demonstrate which are the most commonly used. This will allow a better comprehension of the work proposed in this dissertation, as well as giving insight about the work being develop in this area.

3.1 3D Printed Electrodes for EMG

Jonathan Lévesque et al. [41] designed 3D printed electrodes for monitoring EMG signals. In order to do so, three different materials were tested as support materials: TPU, PLA and Acrylonitrile Butadiene Styrene (ABS). As conductive material, the conductive versions of the filaments listed were used. Besides, they also tested electrodes with the same materials but with the application of gold-plating in order to improve the interaction between the skin and the electrode. For the printing process, to print with both filaments simultaneously, it was used a dual extruder printer. The results shown that the signal obtained using TPU and PLA had the less noise from the three options during the signal acquisition. In Figure 3.1, it is possible to see the design chosen for these electrodes, with the conductive part being circular and the support part having an oval shape.

G. Wolterink et al. [81] created an electrode fabricated through additive manufacturing, using non-conductive and conductive TPU as support material and active layer. The device resembles a bracelet with four points of conductive material in contact with the skin.

Using conductive TPU, Wolterink [82] also developed snap button-like electrodes to measure EMG which were also built using additive manufacturing. The device was tested on a group of volunteers, who performed a set of arm and hand movements with the manufactured electrodes and commercial electrodes to compare the results. The data showed that this filament had the potential to be used for producing flexible electrodes for EMG monitoring as well as other biosignal measurements, such as ECG.

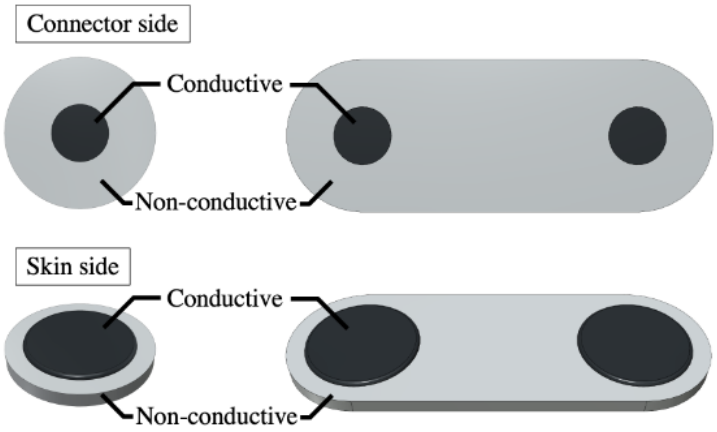

Figure 3.1: Design of a 3D Printed Electrode made using TPU as support material and conductive TPU as conductive material. Adapt From: [41]

3.2 Self Adhesive and Self Standing Electrodes for EMG

Self-adhesive electrodes, which do not need any adhesive to adhere to the skin, are reusable and less likely to cause allergic reactions. Mimicking animal patterns were introduced by Yeon Soo Lee et al. [40] and by Da Wan Kim et al. [36]. Both authors applied biomimetics, a concept that uses nature and animal patterns, and applied them to human technologies in order to find solutions for some challenges [23]. Yeon Soo Lee replicated octopus suction cups to create a silicon wet self-adhesive electrode that is able to collect biosignals of EMG and ECG. Regarding the latter, the group used both octopus-like suction cups, as well as amphibian-like membranes with hexagonal arrays, to create ECG electrodes that adhere to skin.

Besides the patterns based on frog paw pads and octopus suction cups, hexagonal-shaped microchannels were incorporated in the electrode architecture, as can be seen in Figure 3.2, for water drainage which provided better adhesion between the electrode and the skin, and consequently better performance.

Using a layer of gold between two layers of parylene, Robert A. Nawrocki et. al [56], created a self-adhesive dry electrode that allows biopotential monitoring. Every layer has a 10 nm height, making the sensor lightweight and very comfortable. The results show that it can be used to monitor EMG and ECG. The self-adhesiveness comes from perspiration, since it creates surface tension, allowing the electrode to adhere to the skin.

3.3 3D Printed Electrodes

TPU is a flexible thermoplastic that offers great mechanical and thermal resistance [19]. Additionally, it is biocompatible, which makes it an interesting option to use for 3D-printed electrodes for recording electrophysiological signals. Yan Li et. al [42] utilized this material to print wearable pressure sensors. To create the filament, they used a mix of TPU pellets

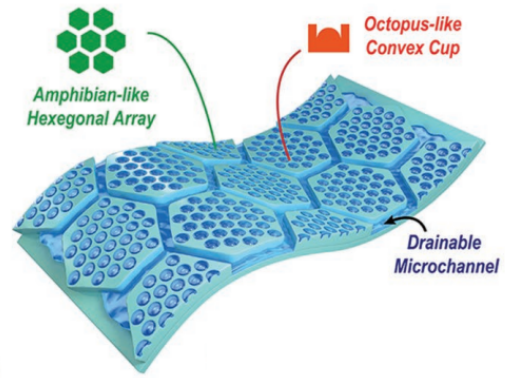

Figure 3.2: Self-Adhesive Electrode with amphbian-like patterns and octopus-like suction cups. Adapt From: [36]

with Dimethylformamide. After printing, the sensor was coated with graphene oxide as well as Silver nanowires, creating a fine sheet with about 0.98 nm thickness. This layer provides better sensitivity and range of detection compared with other pressure sensors.

3.4 Summary

In Table 3.1, it is presented a summary of the most relevant features of each electrode described in this chapter. The table shows the methods of fabrication, materials used, self-standing and self-adhesive characteristics.

After carefully analyzing the electrodes above described, it is possible to see that the self-adhesive electrodes were not fabricated using 3D printing. The electrodes fabricated using additive manufacturing used as active material a conductive filament. For this work it is intended to create a self-adhesive electrode, using additive manufacturing, with TPU as support material.

The next step was to start sketching the first models of electrodes we want to test, we will explain in detail in chapter 4.

3D printed	Conductive Material	Support Material	Self-Adhesive	Reference
Yes	Conductive PLA	PLA	No	[41]
Yes	Conductive ABS	ABS	No	[41]
Yes	Conductive TPU	TPU	No	[41]
Yes	Conductive TPU	-	No	[82]
No	-	Silicon	Yes	[36]
No	Gold	Parylene	Yes	[56]

Table 3.1: State of the Art for EMG Electrodes

4

Materials and Methods

In this chapter, it will be described the fabrication process used to produce EMG electrodes to record the activity of both the bicep and tricep using additive manufacturing. The sketch of the electrode prototype will be presented followed by the manufacturing using Fused Deposition Modelling (FDM) of the different components. Next, it will be presented multiple tests conducted with different materials to find the best method for the conductive part of the electrode. Afterwards, we will also discuss the techniques used for the electrode and material characterization, to better understand the proprieties of the filaments used, such as constitution, conductivity, and impedance and to comprehend the behaviour of the electrode itself when measuring the EMG signal.

Firstly, we will present the materials chosen for the prototype, then the entire process of the sketch and the printing of the electrodes is going to be explained, as well as the procedures to achieve a conductive layer on the models until the final prototype was accomplished. Finally, we conclude this chapter by describing the tests done on the electrode prototype.

4.1 Materials

One of the most common materials used as filament in FDM is Polylactic Acid (PLA). This material possesses unique characteristics that make it widely appealing for this process [53]. Moreover, it is simple to print, is easily found with different colours and diameters, and overall is a quite low-cost filament. However, PLA is a rigid material and consequently can not be used to create a comfortable electrode that can adapt to the shape of the patient's arm. So,TPU was chosen as the base material for the electrodes to be developed. TPU is a flexible thermoplastic that is affordable and presents high durability and corrosion resistance. It is also recyclable and compatible with most printers.

We started this work by using an Ultimaker White TPU 95A filament, with a diameter of 2.85 mm. Despite that, the filament had to be changed during the work since it was necessary to swap printers, which lead to some prototypes being printed using Red and Green TPU FilaFlex 82A, with a 1.75 mm diameter. It was also utilized a conductive

filament, in this case, Black Conductive FilaFlex which also presents a diameter of 1.75 mm.

4.2 3D Printing Process

In this section, the 3D printing process will be present along with the printing tests of biommimetic-like patterns performed. Starting by octopus suction cups, to suction cups with domes, bracelet like designs, until the final prototype is achieved.

FDM is one of many additive manufacturing techniques that was first patented in 1988 by Crump [77]. The complete process that is required to use this method can be observed in Figure 4.1. It starts with the design of the desired object in a specialized software which supports the CAD format, then converted to STL format, and finally sent to the printer.

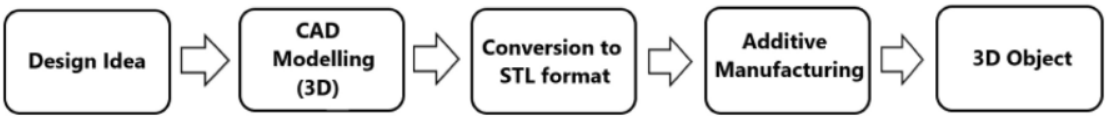

Figure 4.1: Complete process for the additive manufacturing process, from the sketch of the design until the final print is completed. Source: [65]

This technique is one of the most efficient, by having a faster production model, so the relation cost-effectiveness is better when compared to traditional fabrication methods. Due to this, its demand is rising in areas related to medicine, biomedical engineering and many others [47].

The FDM process has a base melt extrusion, where a filament is melted until a molten state, which is then extruded by the nozzle of the printer. The nozzle can move in three degrees of freedom, and therefore create 3D objects, by depositing the extruded material. The filament is consistently fed into the machine's extruder and nozzle by two rollers that are rotating in opposite directions [53]. On the build plate/platform, the material is deposited layer by layer, by either the platform going down or the printer head moving up exactly one layer of thickness until the desired final product is attained. Due to this, it is possible to find an accumulation of material on the edges and the internal region of the outline, which needs to be removed after the printing process is over [77].

The percentage of infilling dictates how full the printed object will be. If it is zero it means the object is hollow inside, while if it is one hundred is a filled object. To achieve a good flexibility the infill can not be high, according to the literature, for best results, the values should range from 10 to 20 % [31]. For the prototypes printed, it was tested infills between 10 and 25%, since one of the main goals was to have a flexible device.

The infill can have different patterns, with the most used ones being linear, hexagonal and diamond. These patterns influence how the nozzle fills each layer [2]. However, these infills are not recommended for more flexible designs. The alternatives chosen to test and

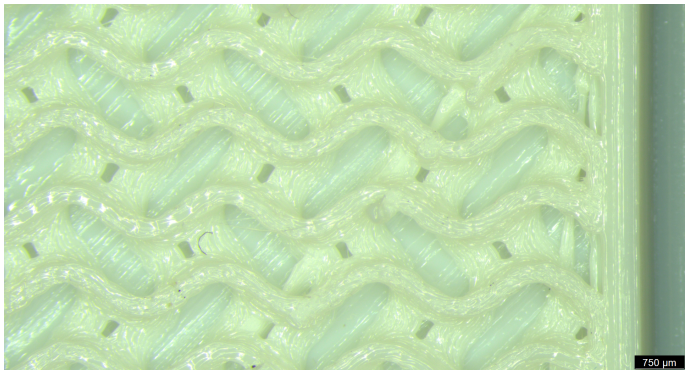

Figure 4.2: Representation of the infill pattern Gyroid

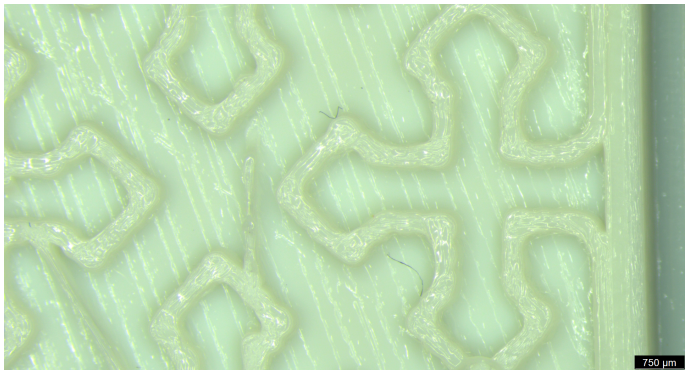

Figure 4.3: Representation of the infill pattern Cross

use were the Gyroid and Cross infills, which are the patterns that offer the best flexibility [18], and are demonstrated in Figures 4.2 and 4.3. Since the gyroid infill gave the final product better flexibility, it was decided to use it instead of the cross infill.

The FDM process can be influenced by several factors, which can be divided into material-related and printer-related conditions. Material properties can be thermal, physical, chemical or mechanical, and influence how the filament can be printed. On the opposite, printer parameters are more diverse, and include the filament characteristics for a perfect print: a final object without any gaps of material or contamination of other filaments, with an outside that is smooth and does not present extra filament. It is necessary to combine the properties of both printer and material to define the optimal parameters for printing, which include, among others, the temperature of extrusion, the building plate temperature, the percentage of extrusion and the printing velocity.

4.2.1 Octopus Pattern

Inspired by biomimetics, the starting point was designing suction cups that mimic the octopus tentacles suction cups in order to create a self-adhesive prototype. The first step was to use *Fusion 360* to draw the sketch. The prototype sketch had 4 mm of thickness, 18 mm of length and 50 mm of width, with the file being saved as STL. The suction cups were circular perforations with a diameter of 5.60 mm and 3.50 mm of depth, with small

half-spheres inside them with a diameter of 4.0 mm, according to the work of Sungwoo Chun et. al [17]. Afterwards, using *Cura* Software, the printing parameters were defined and, then, sent to the printer. At the beginning of the project the printer used was an Ultimaker S2 [1]. However, the nozzle of this printer has always clogging, obstructing the filament and stopping the printing process. This happened due to an incompatibility of the printer with the filament, due to the high flexibility of the TPU. As a result, printing tests were performed on a Ultimaker S3+ [2]. As can be seen in Figure 4.4, the parts printed using this equipment presented much better quality. It is possible to see that without the blockage of filament, the final model does not present any gaps of material and the details have better definition, which translates into an overall better quality of the model printed, with a more accurate representation of the design sketched. As such, the following tests were performed using Ultimaker S3+.

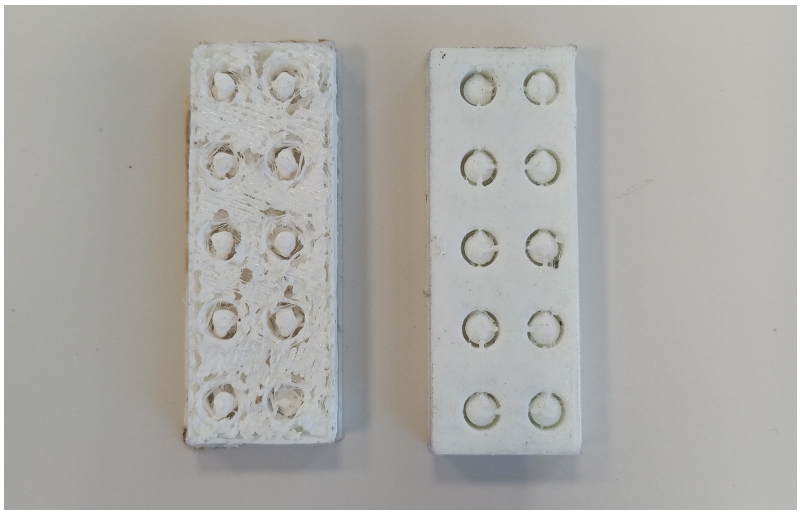

Figure 4.4: Octopus-like suction cups, on the left, printed by Ultimaker S2+, with visible flaws. On the right, the same model was printed by Ultimaker S3, with a much smoother and defined surface. The dimensions of both models are 18 mm in length and 50 mm in width.

The Ultimaker S3+ parameters were optimized and the conditions that yielded, which resulted the best models printed, are presented in Table 4.1 Regarding the adhesion of the prototype, it did not present self-adhesive properties probably due to the high dimension of the patterns resulting from the printing process resolution. As so, tests with other biommimetic-like patterns were performed, namely octopus-like suction cups were printed using the same material.

4.2.2 Suction Cups

The next step was to create self-adhesive suction cups. Firstly, the sketch was modified in order to reduce the thickness of the model, to allow more flexibility and conformity with

[1] Ultimaker S2 - https://newatlas.com/ultimaker-2-3d-printer-speed-accuracy/29268/
[2] Ultimaker S3+ - https://ultimaker.com/3d-printers/s-series/ultimaker-s3/

Printing Parameters	
Built Plate Temperature	0ºC
Nozzle Extrusion Temperature	223ºC
Infill Percentage	20%
Infill Pattern	Gyroid
Ironing 3D	Off
Print Speed	30 mm/s
Nozzle Diameter	0.4 mm

Table 4.1: Ultimaker S3 FDM Parameters

the patient's body. The overall design was also adjusted, by increasing the diameter of the suction cups, to have a bigger area where the electrode could adhere to the skin. The measures used were between 1.35 and 2 mm in thickness, which corresponded to half of the values first tested in the octopus-like suction cups, and the diameter of the suction cups range was varied between 9 and 15 mm, with a conic shape perforation. The first prints were made with just one suction cup, with a diameter of 15 mm to adjust the sketch, then, it was added more suction cups by reducing their size until the final diameter of 9 mm was reached. This decrease in diameter allowed to have more suction cups in the same electrode, providing a better adherence to the skin. The next step was reducing the thickness of the prototype, until the best results were achieved at 1.35 mm of thickness, with four suction cups with 9 mm of diameter, this model was able to adhere to the skin for a longer period, compared with the previous models. It was not possible to reduce even more these measurements since the prototype became to fragile, due to less material being deposited during the printing process. In Figure 4.5, it is possible to see some of the best prototypes achieved with one to four suction cups.

To enhance the adherence, the prototype was printed upside down in order to create a smoother surface. This difference can be seen in Figure 4.6. When printed upside down the surface becomes much smoother since it stays compressed between the printing bed and the rest of the model and there is not any extra filament deposition, this way allowing a better adherence to the skin. Although there was some adhesion, especially on wet skin, it was not enough to achieve the primary objective since the products did not adhere enough to stay on the skin for more than a few seconds.

Intending to create a more stable adhesion, a dome was added on top of each suction cup. Multiple dimensions of the dome were tested, with different heights and thickness, as shown in Figure 4.7. By changing its height between 0.1 and 0.5 mm, the thickness between 0.2 mm and 1.0 mm and keeping the diameter of the suction cup at 9 mm (this diameter value corresponded to the best adhesion results previously tested), multiple versions of the domes were used by combining these three parameters to find the best

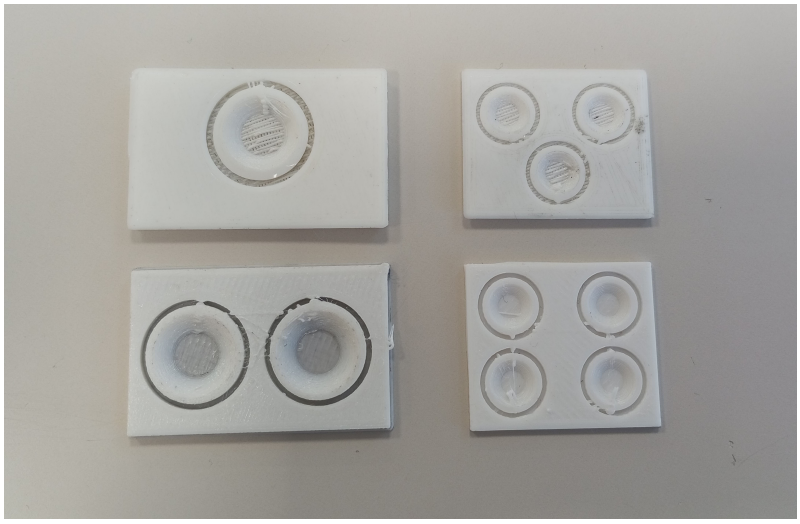

Figure 4.5: Octopus-like suction cups with diameters varying between 9 and 15 mm. On the left side, on the top, one single suction cup is shown with 15 mm in diameter. On the bottom are represented two suction cups with a diameter of 13 mm each. On the right side, on the top of the figure are represented three suction cups with 11 mm of diameter. On the bottom right is the best prototype achieved with this design, with 9 mm of diameter and four suction cups.

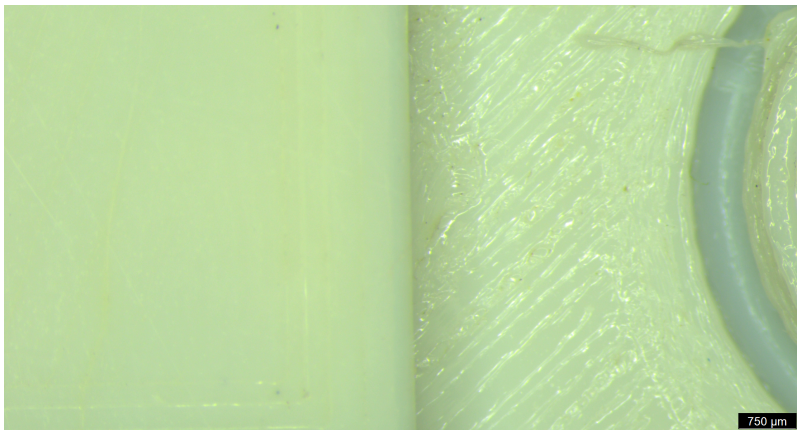

Figure 4.6: Surface Comparison on two prototypes: on the left, the prototype was printed upside down, which led to the smooth surface shown. On the right side is represented the prototype printed normally, which left the top layer with irregularities.

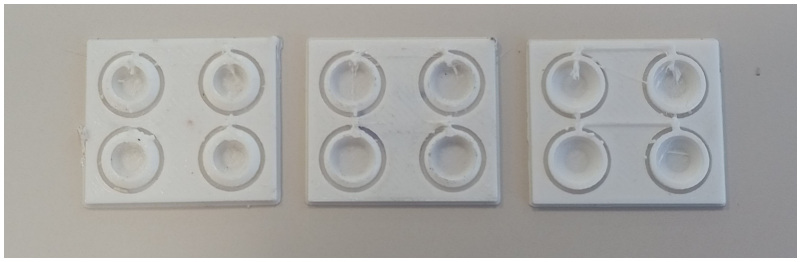

Figure 4.7: Octopus-like suction cups with 9 mm of diameter and domes of thickness of 1.0 mm, 0.5 mm and 0.2 mm, respectively

combination. The best results were achieved with a height of 0.3 mm and a thickness of 0.2 mm. The printer could not print with the precision needed the domes with lower heights. The domes with higher heights and increased thickness resulted in a more rigid model, that did not offer enough flexibility to adhere to the skin. Overall, the adhesion to the skin did not improve, and in some cases, with the higher thickness, it was worsened, due to the loss of conformability with the skin.

Considering that with the domes it was not possible to print the model upside down, to create a more even surface the ironing feature of the printer was tested. This feature adds a top layer to the prototype, filling any gaps left by the print, and then uses the nozzle heat to melt the top surface forming a more regular and smooth surface. However, the use of this feature did not produce the intended results as the final pieces lost some definition and did not contribute to a smoother surface. Instead, the nozzle left a few burn marks on the material, worsening the adhesion of the prototype due to the burned material on the surface of the models.

The results of the tests performed with the suction cups prototypes revealed the need to have more flexible models which can be achieved by decreasing their thickness. More flexibility would then translate into a higher adhesion to the skin. However, a decrease in thickness results in a more complex printing process. Since the sketch has smaller dimensions, the printer needs to have a better resolution. The printers available were not able to print with such detail, thus it was not possible to improve the suction cup designs. For this design to work it was needed a printer with a higher resolution.

4.2.3 Amphibian Pattern

Still inspired by biomimetics, the next attempt combined the previously designed suction cups with some hexagonal shapes characteristic of amphibian paws. According to the literature [52], this shape should form some channels, and create a surface tension, that should provide good adhesion to the skin. First, a model with hexagonal forms with a side of 7.5 mm in length was created. Then, it was placed the suction cups with 9 mm of diameter in the centre of each. With this first experiment, it was possible to conclude that the overall design, both the hexagons and the suction cups, should be smaller, otherwise the model would not adhere to the skin properly.

Afterwards, the size of both the hexagons and the suction cups was reduced, with the length of each side of the hexagon fixed at 3.5 mm and the diameter of the suction cups at 1 mm. However, the printer did not have the precision necessary to print this prototype, as can be seen in Figure 4.8. The suction cups resulted in small perforations. It was concluded that this was not a realistic path to follow, and could only be followed if the proper material and printer were available since it was necessary to use a smaller design that the printer could print with precision. Additionally, the material used (TPU) did not have the flexibility needed for the adhesion effect.

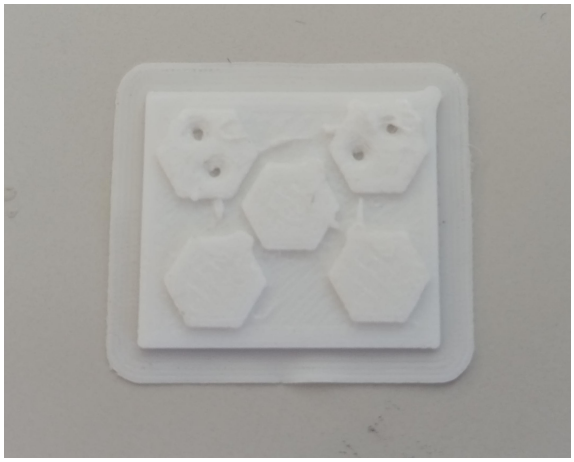

Figure 4.8: Prototype of amphibian pattern with a side of 3.5 mm, with suction cups of 0.1 mm of diameter.

4.2.4 Self-Standing Electrodes

After testing self-adhesive electrodes, a new approach was considered and a self-standing electrode was planned and designed. To do this, first, a sketch of a bracelet-style electrode with a circular shape was made, with the dimensions of 50 mm in diameter, 2.5 mm in thickness and 15 mm in height. The results were quite promising, so the next step was to add a local to insert a ribbon in order to guarantee that the model stayed properly secured to the body of each patient. To achieve this, two small circular perforations were added with 5 mm of diameter each. After some testing, where the model was placed on the body of a volunteer, confirming the ability of the prototype to stay secured in the arm, during movements of extension and flexion of the member, it was concluded that this was the best design to use. The following step was to create a conductive layer on the model, to be able to capture the electrophysiological signals, due to their electrical character.

4.3 Conductive Layer

Having completed the design of electrode support, the next task was to define an approach to create a conductive layer. In this section, three methods to create said layer will be described.

4.3.1 Laser Engraving

The initial approach was laser engraving on the support material of the electrode: TPU. The first equipment used was the CO2 Laser System VLS3.50 [3] with a wavelength of 10.6 microns, a laser with the maximum power of 50 W and available lenses 2.0 in (51 mm). The tested parameters varied from 5% to 30% of power which corresponds to values between 2.5W and 15 W and 5% to 30% speed with values between 0.0127 mm/s and 0.07366 mm/s. Multiple combinations of these values were tested, starting with 5% of power and 5% of speed, going up until 30%. However, there was no visible carbonisation of the TPU and only melting of the material was observed. These results were associated with the thermal sensitivity of the material.

As so, the next step was impregnating the surface of the TPU with a fire-retardant to increase its thermal resistance. First, an aqueous solution of sodium tetraborate decahydrate $Na_2[B_4O_5(OH)_4 \cdot 8\,H_2O]$ from Sigma-Aldrich with a concentration of 0.1 M was prepared. Then, TPU was heated to 93ºC to enhance the adhesion of the fire-retardant to the polymer and the printed piece was submerged in the sodium tetraborate solution for 30 minutes and dried for 24 hours. Afterwards, the treated TPU was exposed to laser radiation using the same conditions mentioned before, however, no graphitization occurred which could be ascribed to the low sensitivity of the material to the laser wavelength [15]. The results were not as expected, even though this time the material did not burn, it was just slightly melted.

Next, a Laser System PLS6MW [4], a fiber laser, with a wavelength of 1.064 microns, maximum power of 50 W and available lenses 2.0 in (51 mm). was used for testing the raw and impregnated in the sodium tetraborate solution TPU, using the same parameters described earlier on the CO2 Laser System VLS3.5. Both the raw and fire-retardant treated TPU did not present any changes after being laser exposed indicating that laser engraving in TPU was not a viable method to create a conductive surface.

4.3.2 LIG Electrodes

As no LIG could be produced from the TPU substrates, a transfer method previously reported in the literature [61], was tested. Based on already developed methods [59], the CO2 Laser System VLS3.50 with parameters of 12% of power and 12% of speed were utilized on paper previously treated with wax and impregnated with a sodium tetraborate solution. Then it was transferred to the TPU using a water transfer technique. The method used consists of placing the paper with the graphene upside down in the TPU, then submerging it in water and slowly removing the paper from the TPU model, leaving the

[3] CO2 Laser System VLS3.50 - https://www.cenimat.fct.unl.pt/lab-facilities/thin-film-lab/laser-system-vls350-cutting-and-engraving-machine

[4] Laser System PLS6MW - https://www.cenimat.fct.unl.pt/lab-facilities/thin-film-lab/laser-system-pls6mw-cutting-and-engraving-machine

graphene attached to the TPU surface. To improve the adherence between the paper and the TPU, it was used an adhesive spray before the transfer process.

Even though a homogenous LIG lase can be produced on top of TPU, the LIG electrodes are quite sensitive, and the slightest movement can cause tear and create gaps in the graphene material, as shown in Figure 4.9. As one requirement of the developed wearable electrodes is flexibility, the material of the conductive part of the electrodes has to present a good mechanical resistance so the transfer process was disregarded as the LIG transferred to the TPU support material present cracks after the electrodes were used for a few minutes.

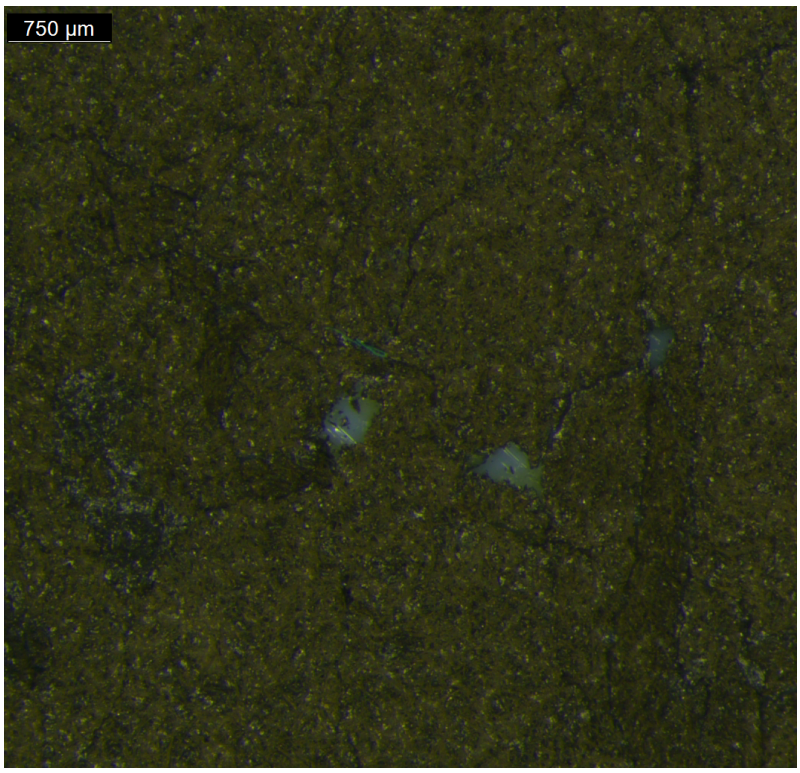

Figure 4.9: Damage in LIG electrodes. The material shows cracks and loss of material. In some areas the LIG was completely removed, leaving the white TPU showing.

4.3.3 Conductive Filament

The next step was to try to use only additive manufacturing for the construction of the electrode, including the conductive part. For this, a new design of the bracelet was sketched, including a designated area for conductive material to be inserted. This can be seen in Figure 4.10 with the colour white as the TPU bracelet, and with the colour orange, the conductive part, made with conductive FilaFlex.

To print this prototype, it was needed a double extruder printer with two nozzles, and that was compatible with the conductive filament, which has a diameter of 1.75 mm. Although the printer Ultimaker S3 has a double extruder, it was not compatible with the filament, since it only accepts filaments with a diameter of 2.85 mm. Instead, the printer

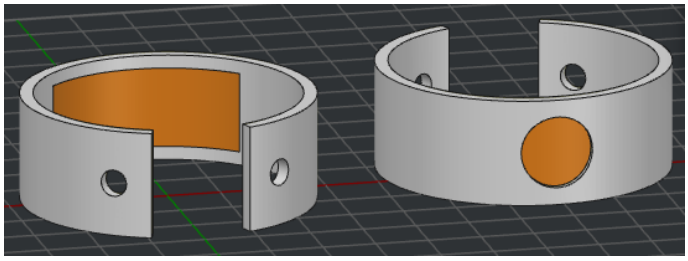

Figure 4.10: Self-standing electrode with TPU (white) as support material and the conductive layer (orange) with conductive FilaFlex. The model is 50 mm in diameter, 2.5 mm in thickness and 15 mm in height

Printing Parameters	
Built Plate Temperature	0ºC
Left Nozzle Extrusion Temperature (TPU)	245ºC
Right Nozzle Extrusion Temperature (Conductive Filament)	245ºC
Infill Percentage	15%
Infill Pattern	Gyroid
Print Speed	40 mm/s
Nozzle Diameter	0.4 mm

Table 4.2: Raise3D E2 FDM Parameters

used was Raise3D E2 [5]. This printer presents two independent extruders, which allow to use two different filaments in the same print. The nozzle is compatible with filaments of 1.75 mm in diameter. The built plate can reach 110 ºC and the nozzle has a maximum temperature of 300 ºC. The process of finding the best print parameters was done and in Table 4.2 we can see that some parameters have different values from the previously used printer, including the extrusion temperature that was raised to 245 ºC, as well as the printing speed that was increased to 40 mm/s, finally, the infill percentage was lower to 15%. After a few tests, it was possible to conclude that this was a promising approach, since it kept the process low-cost, was easy to manufacture and the final product was comfortable, adjustable and practical to use.

To allow further testing it was added a place for a snap button into the model to make it possible to connect cables and devices.

4.4 Final Prototype

After some initial tests, it was concluded that the previous design had some aspects that could be improved, so some adjustments were made to enhance the performance. Firstly, the thickness was decreased to provide even more flexibility and conformability to the

[5] Raise3D E2 - https://www.raise3d.com/e2/

body. Then, the conductive part should not be at the same level as the TPU part, instead, it should be higher to guarantee better contact between the skin and conductive filament. To solve this, instead of having a hole where the conductive part fit, it was placed on the surface of the TPU. Finally, after an impedance study (explained in detail in Section 5.2.2), to decide the best dimensions for the conductive part, the final prototype was designed. Having in mind the importance of the individual study of different muscular groups, a second conductive part was added, in order to make it possible to monitor two muscles at the same time.

The final dimensions of the bracelet part, made of TPU, had 260 mm of length, 20 mm of height and 0.7 mm of thickness. This bracelet had two holes with 5 mm of diameter to pass a ribbon, in order to adjust the device to the body of each patient. Also, two additional holes were made to accommodate two snap buttons, one for each arm muscle. The conductive parts, made of Conductive FilaFlex, had 50 mm of length, 15 mm of height and 2 mm of thickness. Since the main goal was to measure the activity of two muscles the prototype had two of these conductive parts. The final prototype can be seen in Figure 4.11. It is also relevant to mention that the TPU used for the final product was red because the green used initially showed some defects when printing.

To glue the snap buttons to the electrode, it was used commercial silver ink (AG-510 silver ink, Conductive Compounds, Inc., Hudson, NH). The application of the ink was made using a brush, and the electrode was placed in the oven at 50 ºC for two hours to dry.

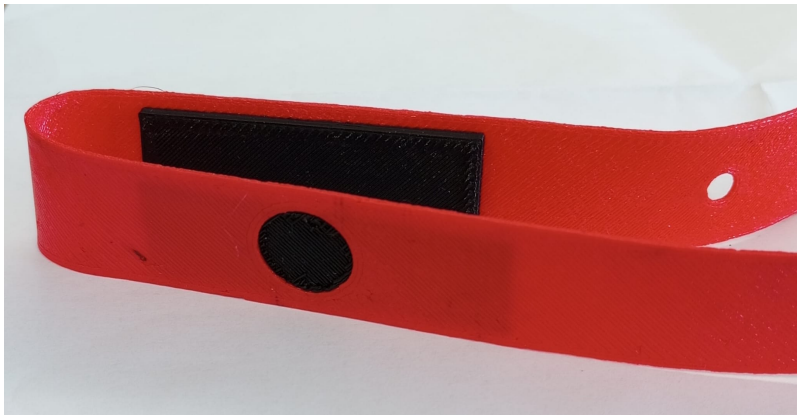

Figure 4.11: Final Prototype of the self-standing electrode for EMG monitoring. The model has 260 mm of length, 20 mm of height and 0.7 mm of thickness

4.5 Characterization Methods

In this section, we will explain the methods used for material and electrode characterization such as sheet resistance, raman and impedance spectroscopy.

4.5.1 Sheet Resistance

To study the electrical properties of the materials used to produce the wearable electrodes their sheet resistance was measured using the *HL5500 Hall effect system*. The samples evaluated were squares with dimensions of 1.5 x 1.5 mm. The conductive Filaflex sample had a thickness of 1 mm, and the TPU 2.5 mm. The sheet resistance was calculated by the equation below [54], where SR corresponds to Sheet Resistance (ohm/sq), R to Resistance (ohm) and t the thickness of the material (mm):

$$SR = \frac{R}{t}$$

4.5.2 Raman Spectroscopy

Since the filaments used for this work were both commercial, to study their composition and what type of carbon was the conductive filament made of, and to verify if the TPU had any other elements, it was utilized a *Raman Microscope – Reninshaw Qontor*, with a spectral resolution of 0.3 cm-1 and 100 nm of lateral resolution to perform Raman Spectroscopy in samples of both materials. The parameters used for the analysis are shown in Table 4.3.

Raman Parameters	
Laser Wavelength	532 nm
Power	1%
Accumulations	3
Objective	20x

Table 4.3: Raman Spectroscopy Parameters

4.5.3 Impedance Spectroscopy

Impedance studies were performed using electrodes with different designs to evaluate their influence on the properties of the final prototype. The impedance is influenced by the area and the thickness of the material, so different electrodes were designed with three distinct areas: 450, 600 and 750 mm2 and three thickness values: 1.50, 2 and 2.50 mm, combining these two parameters into nine prototypes. It was also used a pea size in each electrode of electrolyte gel, The study was made using *PalmSens4* with a current range of 100 uA. The objective was to better understand which was the best area and thickness to use in the final product. It was used one commercial electrode of Ag/AgCl as a reference, to reduce the signal noise, and two prototype electrodes with a distance between them of 2.5 cm.

4.6 Summary

To achieve the bracelet style, first we tried different designs: beginning with a octopus pattern model, trying to recreate the suction cups seen in octopus tentacles, which did not offer enough flexibility to the prototype. Then, a different design of suction cups were tested. This time we achieved better results, the model presented some adhesiveness, specially in wet skin. Afterwards, some domes were added to the previous model to try enhance the adhesion which did not work as expected, with an adhesion decreasing instead. Still following a biomimetric approach, a model that resembled amphibian paws with an hexagonal shape combined with the suction cups without the domes, was tested. The conclusion taken was that the printer did not present enough resolution to give the detail needed for the model to work correctly, so another approach followed. Next, it was tested a self standing, bracelet style model, which obtain overall satisfying results. To achieve even better results we added a ribbon to keep the model secure during the patient movements.

After finding the best design for the electrode, the challenge was to create a conductive surface in the electrode. To do so three different approaches were tested. The first one was to submit the TPU itself to the laser, and trying to create LIG electrodes. However, even with a fire retardant solution impregnated in the material, it was never possible to achieve any type of carbon ligament necessary for an efficient conductive surface. The following experiment was made with LIG electrodes on paper and only then transferred it to the TPU model. This second experiment has successful in creating a conductive layer, however, due to its fragility, it was not a viable option for the prototype. Finally, the solution chosen was a commercial conductive filament made with carbon. This filament allows the fabrication of the electrode in just one print using a dual extruder printer, making the process faster and simpler.

Having the conductive material decided, it was then carried out an impedance study to identify the best measures for the conductive part in order to have a better interaction between the skin and the electrode. To know more about the commercial filaments used, it was performed a Raman spectroscopy on both as well as sheet resistance measures to better understand the conductive behavior of each of them.

5

Results and Discussion

Throughout this chapter, it will be presented the results obtained from the characterization methods used. Starting with the material characterization, we used Raman spectroscopy to analyze the components of the filaments utilized. Secondly, an electrode characterization was conducted, by performing EMG on two muscles: bicep and tricep. It will also be presented the impedance spectroscopy study, where the influence of material area and thickness was studied. The sheet resistance of the materials was also measured, in order to understand the conductive behaviour of both materials. Lastly, the results of the EMG signal captured using the electrodes fabricated will also be demonstrated.

5.1 Material Characterization

In order to characterize the materials used for the fabrication process, the commercial TPU and the conductive FilaFlex were studied using Raman spectroscopy to assess the chemical bonds present in these materials and consequently their main components.

5.1.1 Raman spectroscopy

Both materials used to fabricate the electrodes of, TPU and conductive TPU, were commercial filaments whose composition is not detailed by the manufacturer. In Raman spectroscopy, when the laser encounters the material, the light is reflected with a different wavelength of the initial laser and has different values for each material. Thus, allowing the identification of the specimen submit to the spectroscopy. This effect is called the Raman Effect and is the base behind the Raman spectroscopy [75, 73]. Through this method, it is possible to identify specific peaks, that will allow finding the components within each filament. In Figures 5.1 and 5.2, it is possible to observe the Raman spectra of TPU and the conductive FilaFlex.

Firstly, in the TPU spectrum, it is possible to observe two main peaks that match the two characteristic peaks of this material at approximately 1615 cm-1 and 2930 cm-1 [20], which allowed to confirm that the main material in the filament is TPU.

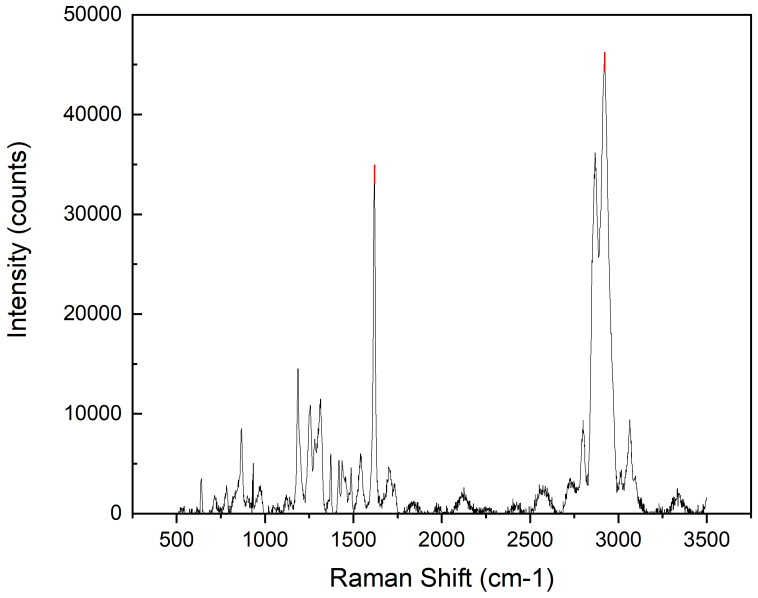

Figure 5.1: Raman Spectroscopy of TPU Filament

Secondly, in the Conductive FilaFlex spectrum, we can see three distinct peaks. Two of them are characteristic of carbon materials: The first one at approximately 1350 cm-1, corresponds to the D-band and the following peak at around 1600 cm-1 matches with the G-band that is located between 1500 and 1600 cm-1 [22]. These two peaks are typically present in the Raman spectrum of amorphous carbon. The third peak at 2925 cm-1, corresponds to C-H stretching, which points to the to the presence of TPU in the filament [27]. These results, lead to the conclusion that the conductive filament is a mix of TPU with amorphous carbon.

5.2 Electrode Characterization

5.2.1 Sheet Resistance

In Table 5.1, it is possible to observe the Sheet Resistance (SR) and the associated Standard Deviation (SD) of both filaments used for the printing process: Conductive FilaFlex and TPU. Three measurements of the same sample were made for which material. The difference between the sheet resistance of TPU and conductive filaflex was notorious. TPU is a non-conductive polymer, as such its insulating properties lead to a high sheet resistance value, as shown in the table mentioned. Regarding the sheet resistance of the conductive filament, although the other material is conductive, it presents a higher resistance, it is several order of magnitude lower than that of TTPU due to the amorphous carbon present in its structure as detected by Raman spectroscopy (Figure 5.2). However, this sheet resistance value is high compared to that of other carbon-based materials such

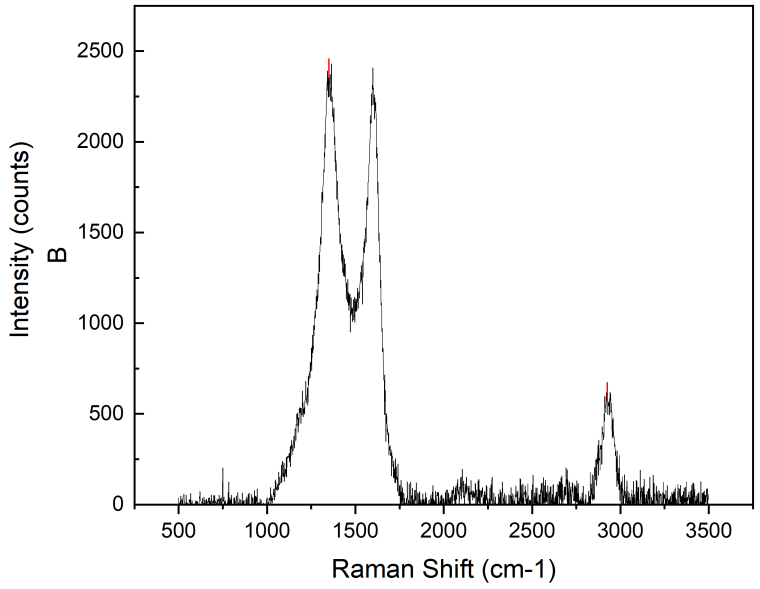

Figure 5.2: Raman Spectroscopy of Conductive Filaflex

as carbon black, which presents a 170 ohm/sq sheet resistance [43]. This difference can be due to other materials that are non conductive being in the filament, such as TPUt or due to the low number of conductive particles being in the filament.

Material	**SR (ohm/sq)**	**Mean SR ± SD (ohm/sq)**
Conductive Filament	896.4 898.6 895.9	897 ± 1
TPU Filament	2.90E+11 2.78E+11 5.09E+11	(4 ± 1) E+11

Table 5.1: Sheet Resistance of Conductive Filament and TPU Filament

5.2.2 Impedance spectroscopy Study

In order to evaluate the interaction between the skin and the electrode, it was performed an impedance study. For this work, it was used three different areas and three different values of thickness which resulted in nine testing conditions for measurements, as shown in Table 5.2.

The measurements were made with two electrodes, placed in the arm with electrolytic gel (Spectra - 360 Electrode Gel) and secured with medical grade tape, as shown in

	1A	1B	1C
Area (mm^2)	600	600	600
Thickness (mm)	1.50	2.0	2.50
	2A	2B	2C
Area (mm^2)	450	450	450
Thickness (mm)	1.50	2.0	2.50
	3A	3B	3C
Area (mm^2)	750	750	750
Thickness (mm)	1.50	2.0	2.50

Table 5.2: Impedance Study: Tested area and thickness combinations

Figure 5.3. Plus, a third commercial Ag/AgCl electrode was placed in the elbow to serve as reference. The electrodes had a distance of 2.5 cm between them since this is the distance between the electrodes for measuring the EMG of the arm muscles. The measurements were conducted with a *PalmSens4* potentiostat. The applied current range was 100 microAmpere and the maximum frequency was set to 5000 Hz.

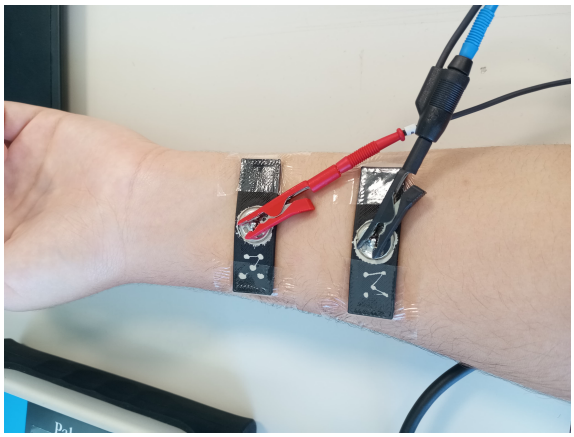

Figure 5.3: Electrodes placement for impedance study.

Impedance depends on multiple variables, such as the area and thickness of the material. The area of the material has an inverse proportion with the impedance, which means that in the study conducted it was expected to see a decrease in impedance when the area was increased. On the other hand, the thickness of the material is directly proportional to the impedance, thus, we expect to observe an increase of impedance when the value of the thickness increases [32, 9, 57].

In Figure 5.4 is represented the graph for electrodes with an area of 600 mm^2, and three different values of thickness: 1.5 mm (1A), 2 mm (1B) and 2.5 mm (1C). Figure 5.5, is relative to the electrodes with an area of 450 mm^2 and three different thicknesses: 1.5 mm (2A), 2 mm (2B) and 2.5 mm (2C). Finally, in Figure 5.6 is demonstrated the results for the electrodes with 750 mm^2 of area and different thickness values: 1.5 mm (3A), 2 mm (3B)

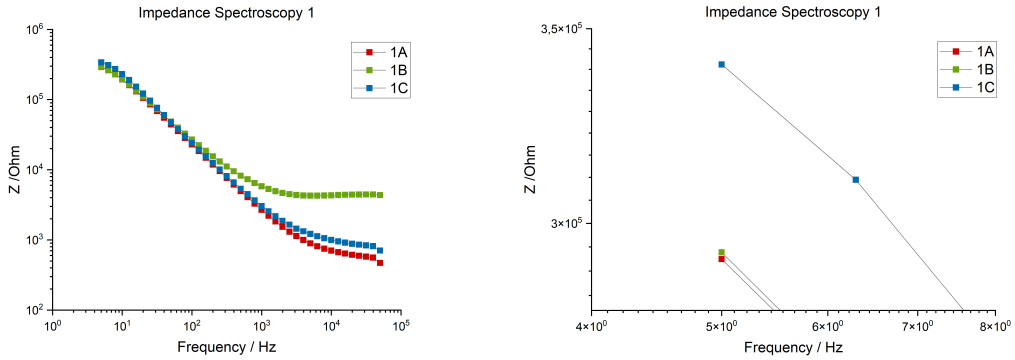

Figure 5.4: Impedance Spectroscopy for the area of 600mm^2 with three values of thickness. On the left the full graph and on the right, zoomed in, to better identify the maximum values.

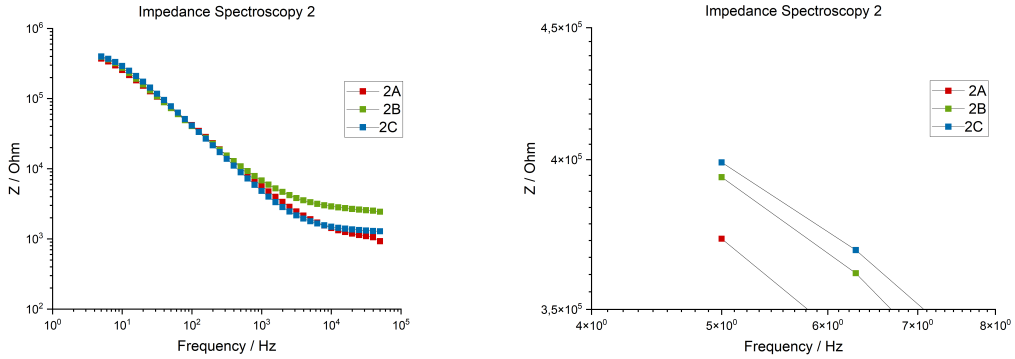

Figure 5.5: Impedance Spectroscopy for the area of 450 mm^2 with three values of thickness. On the left the full graph and on the right, zoomed in, to better identify the maximum values.

and 2.5 mm (3C).

Starting by analyzing the graphs from Figures 5.4, 5.5 and 5.6. The analysis of the graphs presented in Figures 5.4, 5.5 underline the proportional relation between thickness and impendance, as would be expected. As so, it is clear that samples with greater thickness (identified with C) present higher impedance values across the frequency range used for the tests whereas samples identified with A (lower thickness) present lower impedance values.

However when observing the graphs from Figure 5.6, which corresponds to the electrodes with 750 mm^2, this trend is not observed. The sample with intermediate thickness presents the lowest impedance values which can be ascribed to conformability problems.

The 3C prototype presented a high area and thickness, which caused a decrease in flexibility and consequently in conformability. Thus, during the tests the prototype's contact with the skin was not ideal, since it was used medical grade tape to secure it, the tips of the prototype did not have full contact with the skin, which led to a lower

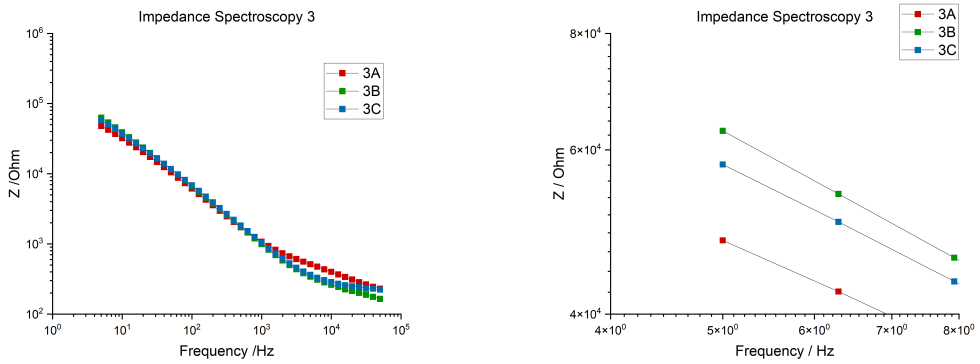

Figure 5.6: Impedance Spectroscopy for the area of 750 mm^2 with three values of thickness. On the left the full graph and on the right, zoomed in, to better identify the maximum values.

effective area. Decreasing the electrode area, led to an increase in impedance since these two measurements are inversely proportional [24].

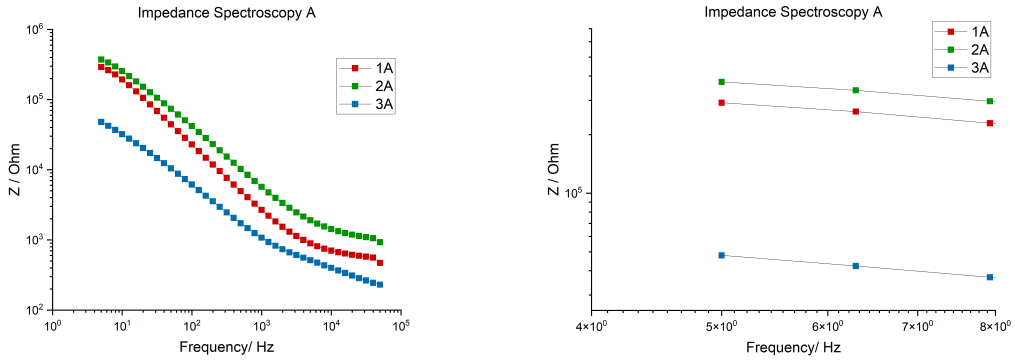

Figure 5.7: Impedance Spectroscopy for 1.50 mm of thickness with three values of area. On the left the full graph and on the right, zoomed in, to better identify the maximum values.

Now, the prototypes with the same value of thickness but with distinct values of area will be compared. In figure 5.7, we can see the results for a thickness value of 1.50 mm and three distinct values of area: 450 mm^2 (2A), 600 mm^2 (1A) and 750 mm^2 (3A). The same is demonstrated in Figure 5.8, but with a thickness of 2.0 mm and different area values: 450 mm^2 (2B), 600 mm^2 (1B) and 750 mm^2 (3B). Lastly, in Figure 5.9 is shown the graph for the thickness of 2.50 mm with the areas of 450 mm^2 (2C), 600 mm^2 (1C) and 750 mm^2 (3C).

In Figures 5.7, 5.8 and 5.9 the results of the impedance studies of electrodes with same thickness but varying area are presented. In each graph, 3 sets of data are presented corresponding to the different electrode areas tested, namely 450, 600 and 750 mm^2. When analyzing the graphs presented in these three figures, an inverse proportion between the electrode area and the corresponding impedance is observed. The biggest area, identified as 3 corresponds to the lowest impedance as for the smaller area, identified as 2, is equivalent to the highest impedance across the frequency range tested.

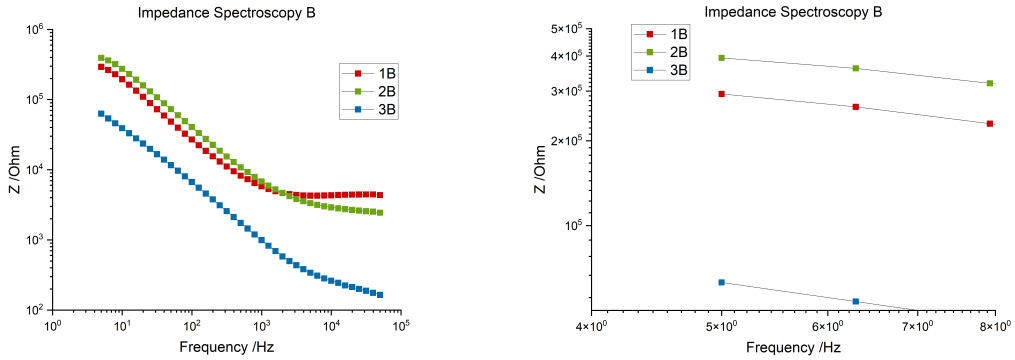

Figure 5.8: Impedance Spectroscopy for 2.0 mm of thickness with three values of area. On the left the full graph and on the right, zoomed in, to better identify the maximum values.

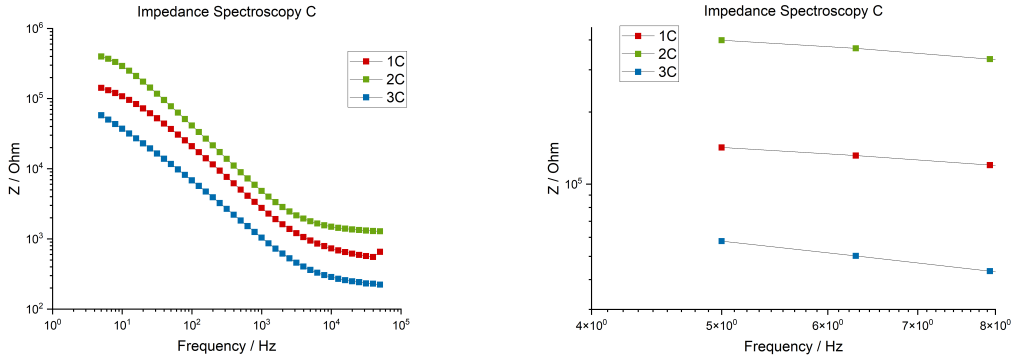

Figure 5.9: Impedance Spectroscopy for 2.50 mm of thickness with three values of area. On the left the full graph and on the right, zoomed in, to better identify the maximum values.

With this experience, it was possible to study the influence of the area and thickness of the produced electrodes on the corresponding impedance values. Regarding the results obtained for varying thicknesses, no significant differences were observed which can be ascribed to the proximity of the thickness values tested. The impedance studies revealed that electrodes with 750 mm^2 area and 2.0 mm thickness presented the lowest impedance values. As such, these were the conditions used to produce the final prototype for multiple EMG recordings of the bicep and tricep muscles.

5.3 EMG Measurement

Evaluating multiple groups of muscle simultaneously is essential to monitor muscle fatigue, as well as to monitor muscle degenerative diseases [48]. To measured the EMG of two muscles, namely bicep and tricep, at the same time, it was used a Bitalino [1] device, one for each muscle. This device can have four sampling rates: 1, 10, 100 and 1000 Hz and has multiple sensors, among them a EMG sensor. The electrodes were placed in the

[1] Bitalino - https://www.pluxbiosignals.com/pages/bitalino?srsltid=AfmBOooN4Qnjl1prNKV3XfyIpC7kAyAmhRK9C3myLse5nK8

Figure 5.10: Electrodes Placement for the EMG of the bicep and tricep.

upper arm of the subject, a female with 22 years old, as shown in Figure 5.10. There was also a reference Ag/AgCl electrode, placed in the elbow. Then, the movement performed consisted of two different steps: first the contraction of the bicep with the arm at 90 degrees, followed by the over-extension of the arm, to activate the tricep, these movements were repeated four times in each measurement.

It was used a sampling rate of 1000 Hz, and the results were processed with the software *OpenSignals*, as shown in Figures 5.11 and 5.12, where the graphs of the EMG signals of both muscles are represented. Observing the signals it is possible to see the activation of each muscle according to the movement performed. When the bicep contracts, the amplitude of the EMG signal increases, due to muscle activation. Although the EMG signal of the tricep presents muscular activity, as spikes above the muscular tonus are visible, but their amplitude is smaller than the bicep EMG. Furthermore, when the over-extension of the arm is performed, the EMG signal of the tricep increases, and the bicep EMG signal decreases until is barely above the muscular tonus level.

The activation of the bicep and the tricep, depending on the movement performed is clearly visible in the EMG recorded using the developed electrodes, as shown in Figure 5.13.

In order to compare the signal obtained with the signal captured by the commercial electrodes, the same movements were then performed, using commercial Ag/AgCl electrodes to capture the EMG signal. The results can be observed in Figure 5.14, the similarities between both signals are easily seen. These results highlight the promising future of the developed electrodes for the detailed monitoring of the muscular activity of different muscles.

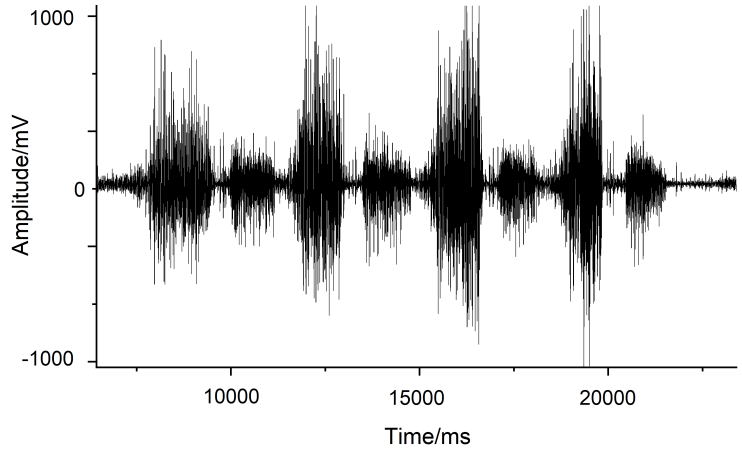

Figure 5.11: EMG signal of the Bicep, during arm flexion followed by overextension of the member. This movement was repeated four times

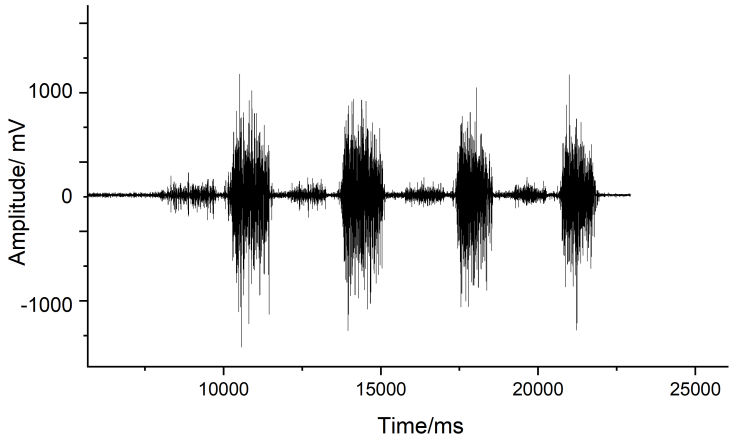

Figure 5.12: EMG signal of the Tricep, during arm flexion followed by overextension of the member. This movement was repeated four times.

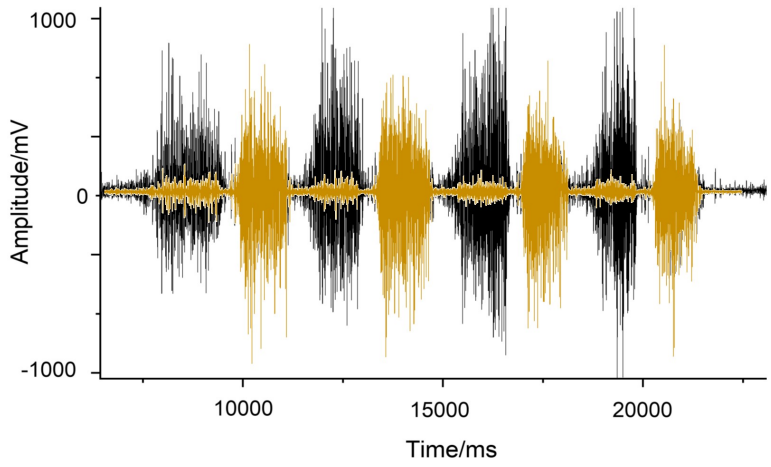

Figure 5.13: EMG signal of the Tricep (Yellow) and the Bicep (Black) overlap during the arm flexion and extension.

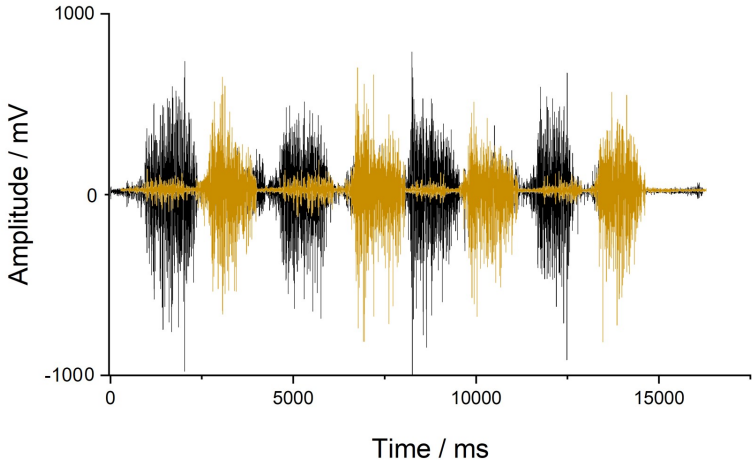

Figure 5.14: EMG signal of the Tricep (Yellow) and the Bicep (Black) overlap during the arm flexion and extension, captured using commercial Ag/AgCl electrodes.

5.4 Summary

In this chapter, the results from the materials and the electrode characterization were demonstrate and explained. Starting with the analyses of the Raman spectroscopy of both filaments used to fabricate the electrode, followed by an impedance study and the determination of sheet resistance values. With these methods, we came to the conclusion that the best measurements for the conductive part of the electrode were an area of 750 mm^2 and a thickness of 2.0 mm. Furthermore, it was also proven that the electrodes fabricated can capture the EMG signal of two muscles at the same time.

6

Conclusion and Future Work

6.1 Conclusion

The main objective of this work was to create flexible and self-standing electrodes that could be used for EMG monitoring. This was achieved by using thermoplastic as base material and additive manufacturing for the fabrication, having a recyclable and reusable final prototype.

Different approaches were tested to produce self-adhesive electrodes, namely different patterns such as octopus-like suction cups, suction cups with domes and amphibian-like patterns were tested. These patterns were produced using TPU. The aim of these patterns printed on the base of the electrode was to provide self-adhesiveness so that it could be reusable. However, the resolution of the printing equipment used to produce these patterns limited the minimal size that could be printed with good definition preventing the printing of patterns small enough for the electrodes to be self-adhesive.

As an alternative to self-adhesive electrodes, a prototype of self-standing electrodes, with a bracelet-like style, was developed using additive manufacturing. TPU was used as support material and conductive filaflex as the main component of the conductive part of the electrodes.

Through Raman spectroscopy, the composition of the filaments was analyzed. The obtained data revealed the main component of the material used to print the electrodes' support was TPU which was also present in the composition of the conductive filament. Regarding the later, Raman analysis demonstrated the presence of amorphous carbon in its composition. By calculating the sheet resistance of each of them it was possible to better understand their conductive behavior. The conductive FilfaFlex presented a sheet resistance above different carbon-based materials, which could occur due to the presence of other materials in the filament, such as TPU. By conducting an impedance study it was possible to understand which dimensions, of the conductive layer, would benefit the interaction between the electrode and the skin. It was tested three different values of thickness (1.5 mm, 2.0 mm and 2.5 mm) and three values of area of the electrode (450 mm2, 600 mm2 and 750 mm2). It was also proven the direct proportion between the thickness

of the material and the impedance values as well as the inverse proportion between the area of the electrode and the impedance. After carefully analysing the results, the lower impedance was obtained with the electrode with 750 mm2 of area and 2.0 mm of thickness.

As a proof of concept, a prototype able to monitor the activity of the bicep and the tricep was developed. The support material was TPU and the conductive part was conductive FilaFlex with an area and thickness of 750 mm2 and 2.0 mm. These electrodes were tested by a subject performing movements that caused the activation of the biceps and the triceps. It was possible to see EMG of both muscles, thereby proving the viability of the devices produced. Besides, since these electrodes are reusable and recyclable, they provide an alternative to the traditional disposable electrodes, reducing this way the single-used devices used in healthcare.

In addition, unlike the additive-manufactured EMG electrodes reported in the literature, the electrodes described in this dissertation do not require any adhesive to adhere to the skin. These devices have a ribbon that allows them to adjust to the patient's arm, demonstrating the high adaptability of the developed electrodes to different users. All these characteristics demonstrate the potential of the proposed electrodes for simultaneous monitoring of multiple muscle groups, presenting themselves as a low-cost alternative for more comprehensive diagnostics.

6.2 Future Work

In the future some adjustments can be made to the developed prototype, in order to enhance the electrode's performance:

- Firstly, more tests to improve the contact between the skin and the electrode can be done, since the signal obtained during the EMG recording had some noise compared to commercially used Ag/AgCl electrodes. The conductive part of the prototype has a rectangle shape and its surface is quite smooth. Moreover, a study about the influence of adding some rugosity or some micro shapes on the top surface of it could be conducted, in order to analyze its influence on the impedance with the skin. Another interesting test could be to evaluate the effect of the shape of the conductive part on the interaction between the electrode and the skin. So, instead of a rectangle, some other shapes could be considered, for example, a circle, a square or even some abstract shape.

- Furthermore, another relevant assessment is to analyze the behaviour of the electrodes without the electrolytic gel that was used for all the measurements in this dissertation. This is relevant since the gel can cause allergic reactions and dehydration during the use of the electrodes. Besides the long use of the electrode with the gel can lead to signal deterioration.

- Having in mind the first designs sketched (octopus-like suction cups and amphibian patterns), which were not possible to pursue due to printer and material incompatibilities, it would also be interesting to test those prototypes using an even more flexible material, such as silicon, and a micro-precision printer.
- It would also be interesting to test the developed electrodes for electrical stimulation tests. In most cases of muscle damage or degenerative diseases, besides the use of EMG to diagnose and monitor the progression of the disease, it is also very common to recommend patients to electrical stimulation therapy. Thus, electrodes with a dual function of monitoring muscle activity and electrical stimulation would be a valuable diagnostic and treatment tool.

Bibliography

[1] H. A. Abdulbari and E. A. M. Basheer. "Electrochemical Biosensors: Electrode Development, Materials, Design, and Fabrication". In: *ChemBioEng Reviews* 4.2 (2017), pp. 92–105. DOI: https://doi.org/10.1002/cben.201600009. eprint: https://onlinelibrary.wiley.com/doi/pdf/10.1002/cben.201600009. URL: https://onlinelibrary.wiley.com/doi/abs/10.1002/cben.201600009 (cit. on p. 7).

[2] A. Alafaghani et al. "Experimental Optimization of Fused Deposition Modelling Processing Parameters: A Design-for-Manufacturing Approach". In: *Procedia Manufacturing* 10 (2017). 45th SME North American Manufacturing Research Conference, NAMRC 45, LA, USA, pp. 791–803. ISSN: 2351-9789. DOI: https://doi.org/10.1016/j.promfg.2017.07.079. URL: https://www.sciencedirect.com/science/article/pii/S2351978917302615 (cit. on p. 14).

[3] A. Ali et al. "Surface electromyography for assessing triceps brachii muscle activities: A literature review". In: *Biocybernetics and Biomedical Engineering* 33.4 (2013), pp. 187–195. ISSN: 0208-5216. DOI: https://doi.org/10.1016/j.bbe.2013.09.001. URL: https://www.sciencedirect.com/science/article/pii/S020852161300034X (cit. on p. 5).

[4] S. Alshammari and B. Bordoni. "Anatomy, Shoulder and Upper Limb, Arm Muscles". In: *StatPearls [Internet]*. [Updated 2023 Jul 24]. Treasure Island (FL): StatPearls Publishing, 2024. URL: https://www.ncbi.nlm.nih.gov/books/NBK554420/ (cit. on p. 5).

[5] A. A. Ansari and M. Kamil. "Effect of print speed and extrusion temperature on properties of 3D printed PLA using fused deposition modeling process". In: *Materials Today: Proceedings* 45 (2021). Second International Conference on Aspects of Materials Science and Engineering (ICAMSE 2021), pp. 5462–5468. ISSN: 2214-7853. DOI: https://doi.org/10.1016/j.matpr.2021.02.137. URL: https://www.sciencedirect.com/science/article/pii/S2214785321011998 (cit. on p. 8).

[6] N. V. R. B. V. Reddy and A. Ghosh. "Fused deposition modelling using direct extrusion". In: *Virtual and Physical Prototyping* 2.1 (2007), pp. 51–60. DOI: 10.1080/17452750701336486. eprint: https://doi.org/10.1080/17452750701336486. URL: https://doi.org/10.1080/17452750701336486 (cit. on p. 8).

[7] M. Bhuvanesh Kumar and P. Sathiya. "Methods and materials for additive manufacturing: A critical review on advancements and challenges". In: *Thin-Walled Structures* 159 (2021), p. 107228. ISSN: 0263-8231. DOI: https://doi.org/10.1016/j.tws.2020.107228. URL: https://www.sciencedirect.com/science/article/pii/S0263823120311009 (cit. on p. 1).

[8] A. Biasiucci, B. Franceschiello, and M. M. Murray. "Electroencephalography". In: *Current Biology* 29.3 (2019), R80–R85. ISSN: 0960-9822. DOI: https://doi.org/10.1016/j.cub.2018.11.052. URL: https://www.sciencedirect.com/science/article/pii/S0960982218315513 (cit. on p. 6).

[9] A. Boyle and A. Adler. "The impact of electrode area, contact impedance and boundary shape on EIT images". In: *Physiological Measurement* 32.7 (2011-06), p. 745. DOI: 10.1088/0967-3334/32/7/S02. URL: https://dx.doi.org/10.1088/0967-3334/32/7/S02 (cit. on p. 30).

[10] C. Brambilla et al. "Combined Use of EMG and EEG Techniques for Neuromotor Assessment in Rehabilitative Applications: A Systematic Review". In: *Sensors* 21.21 (2021). ISSN: 1424-8220. DOI: 10.3390/s21217014. URL: https://www.mdpi.com/1424-8220/21/21/7014 (cit. on p. 2).

[11] P. J. Brewer, R. J. Leese, and R. J. Brown. "An improved approach for fabricating Ag/AgCl reference electrodes". In: *Electrochimica Acta* 71 (2012), pp. 252–257. ISSN: 0013-4686. DOI: https://doi.org/10.1016/j.electacta.2012.03.164. URL: https://www.sciencedirect.com/science/article/pii/S0013468612005312 (cit. on p. 1).

[12] J. R. Camargo et al. "Development of conductive inks for electrochemical sensors and biosensors". In: *Microchemical Journal* 164 (2021), p. 105998. ISSN: 0026-265X. DOI: https://doi.org/10.1016/j.microc.2021.105998. URL: https://www.sciencedirect.com/science/article/pii/S0026265X21000837 (cit. on p. 9).

[13] Y. Cao et al. "Stability study of transition metal oxide electrode materials". In: *Journal of Power Sources* 560 (2023), p. 232710. ISSN: 0378-7753. DOI: https://doi.org/10.1016/j.jpowsour.2023.232710. URL: https://www.sciencedirect.com/science/article/pii/S037877532300085X (cit. on p. 8).

[14] J. Cheng et al. "Locally controllable laser patterning transfer of thermoplastic polyurethane induced by sustainable bismuth trioxide substrate". In: *Applied Surface Science* 550 (2021), p. 149299. ISSN: 0169-4332. DOI: https://doi.org/10.1016/j.apsusc.2021.149299. URL: https://www.sciencedirect.com/science/article/pii/S0169433221003755 (cit. on p. 9).

[15] J. Cheng et al. "Locally controllable laser patterning transfer of thermoplastic polyurethane induced by sustainable bismuth trioxide substrate". In: *Applied Surface Science* 550 (2021), p. 149299. ISSN: 0169-4332. DOI: https://doi.org/10.1016/j.apsusc.2021.149299. URL: https://www.sciencedirect.com/science/article/pii/S0169433221003755 (cit. on p. 21).

[16] T. Cheng et al. "Stretchable Thin-Film Electrodes for Flexible Electronics with High Deformability and Stretchability". In: *Advanced Materials* 27.22 (2015), pp. 3349–3376. DOI: https://doi.org/10.1002/adma.201405864. eprint: https://onlinelibrary.wiley.com/doi/pdf/10.1002/adma.201405864. URL: https://onlinelibrary.wiley.com/doi/abs/10.1002/adma.201405864 (cit. on p. 7).

[17] S. Chun et al. "Conductive and Stretchable Adhesive Electronics with Miniaturized Octopus-Like Suckers against Dry/Wet Skin for Biosignal Monitoring". In: *Advanced Functional Materials* 28.52 (2018), p. 1805224. DOI: https://doi.org/10.1002/adfm.201805224. eprint: https://onlinelibrary.wiley.com/doi/pdf/10.1002/adfm.201805224. URL: https://onlinelibrary.wiley.com/doi/abs/10.1002/adfm.201805224 (cit. on p. 16).

[18] K. Chynybekova and S.-M. Choi. "Flexible Patterns for Soft 3D Printed Fabrications". In: *Symmetry* 11.11 (2019). ISSN: 2073-8994. DOI: 10.3390/sym11111398. URL: https://www.mdpi.com/2073-8994/11/11/1398 (cit. on p. 15).

[19] R. C. Ciobanu et al. "Characteristics of Composite Materials of the Type: TPU/PP/BaTiO3 Powder for 3D Printing Applications". In: *Polymers* 15.1 (2023). ISSN: 2073-4360. DOI: 10.3390/polym15010073. URL: https://www.mdpi.com/2073-4360/15/1/73 (cit. on p. 11).

[20] S. M. Desai, R. Y. Sonawane, and A. P. More. "Thermoplastic polyurethane for three-dimensional printing applications: A review". In: *Polymers for Advanced Technologies* 34.7 (2023), pp. 2061–2082. DOI: https://doi.org/10.1002/pat.6041. eprint: https://onlinelibrary.wiley.com/doi/pdf/10.1002/pat.6041. URL: https://onlinelibrary.wiley.com/doi/abs/10.1002/pat.6041 (cit. on p. 27).

[21] O. Diegel, A. Nordin, and D. Motte. "Additive Manufacturing Technologies". In: *A Practical Guide to Design for Additive Manufacturing*. Singapore: Springer Singapore, 2019, pp. 19–39. ISBN: 978-981-13-8281-9. DOI: 10.1007/978-981-13-8281-9_2. URL: https://doi.org/10.1007/978-981-13-8281-9_2 (cit. on p. 8).

[22] A. Dychalska et al. "Study of CVD diamond layers with amorphous carbon admixture by Raman scattering spectroscopy". In: *MATERIALS SCIENCE-POLAND* 33 (2015-09). DOI: 10.1515/msp-2015-0067 (cit. on p. 28).

[23] P. E. Fayemi et al. "Biomimetics: process, tools and practice". In: *Bioinspiration & Biomimetics* 12.1 (2017), p. 011002. DOI: 10.1088/1748-3190/12/1/011002. URL: https://doi.org/10.1088/1748-3190/12/1/011002 (cit. on p. 11).

[24] W. Franks et al. "Impedance characterization and modeling of electrodes for biomedical applications". In: *IEEE Transactions on Biomedical Engineering* 52.7 (2005), pp. 1295–1302. DOI: 10.1109/TBME.2005.847523 (cit. on p. 32).

[25] V. Gohel and N. Mehendale. "Review on electromyography signal acquisition and processing". In: *Biophysical Reviews* 12.6 (2020-12), pp. 1361–1367. ISSN: 1867-2469. DOI: 10.1007/s12551-020-00770-w. URL: https://doi.org/10.1007/s12551-020-00770-w (cit. on p. 5).

[26] W. Herzog. "Sliding Filament Theory". In: *Encyclopedia of Neuroscience*. Ed. by M. D. Binder, N. Hirokawa, and U. Windhorst. Berlin, Heidelberg: Springer Berlin Heidelberg, 2009, pp. 3745–3748. ISBN: 978-3-540-29678-2. DOI: 10.1007/978-3-540-29678-2_5463. URL: https://doi.org/10.1007/978-3-540-29678-2_5463 (cit. on p. 5).

[27] N. K. Howell et al. "Raman Spectral Analysis in the C-H Stretching Region of Proteins and Amino Acids for Investigation of Hydrophobic Interactions". In: *Journal of Agricultural and Food Chemistry* 47.3 (1999), pp. 924–933. DOI: 10.1021/jf9810741 (cit. on p. 28).

[28] J.-C. Hsieh et al. "Design of hydrogel-based wearable EEG electrodes for medical applications". In: *Journal of Materials Chemistry B* 10.37 (2022), pp. 7260–7280 (cit. on p. 1).

[29] C. Im and J.-M. Seo. "A Review of Electrodes for the Electrical Brain Signal Recording". In: *Biomedical Engineering Letters* 6.3 (2016), pp. 104–112. ISSN: 2093-985X. DOI: 10.1007/s13534-016-0235-1. URL: https://doi.org/10.1007/s13534-016-0235-1 (cit. on p. 1).

[30] S. N. Iwasa et al. "Novel Electrode Designs for Neurostimulation in Regenerative Medicine: Activation of Stem Cells". In: *Bioelectricity* 2.4 (2020), pp. 348–361. DOI: 10.1089/bioe.2020.0034. eprint: https://doi.org/10.1089/bioe.2020.0034. URL: https://doi.org/10.1089/bioe.2020.0034 (cit. on p. 1).

[31] S. L. F. J. H. Porter T. M. Cain and P. S. Harvey. "Influence of infill properties on flexural rigidity of 3D-printed structural members". In: *Virtual and Physical Prototyping* 14.2 (2019), pp. 148–159. DOI: 10.1080/17452759.2018.1537064. eprint: https://doi.org/10.1080/17452759.2018.1537064. URL: https://doi.org/10.1080/17452759.2018.1537064 (cit. on p. 14).

[32] E. S. Kappenman and S. J. Luck. "The effects of electrode impedance on data quality and statistical significance in ERP recordings". In: *Psychophysiology* 47.5 (2010), pp. 888–904. DOI: https://doi.org/10.1111/j.1469-8986.2010.01009.x. eprint: https://onlinelibrary.wiley.com/doi/pdf/10.1111/j.1469-8986.2010.01009.x. URL: https://onlinelibrary.wiley.com/doi/abs/10.1111/j.1469-8986.2010.01009.x (cit. on p. 30).

[33] O. Kaynan et al. "Electrically conductive high-performance thermoplastic filaments for fused filament fabrication". In: *Composite Structures* 237 (2020), p. 111930. ISSN: 0263-8223. DOI: https://doi.org/10.1016/j.compstruct.2020.111930. URL: https://www.sciencedirect.com/science/article/pii/S0263822319345337 (cit. on p. 9).

[34] M. C. Kiernan et al. "Amyotrophic lateral sclerosis". In: *The lancet* 377.9769 (2011), pp. 942–955 (cit. on p. 4).

[35] H.-J. Kil et al. "Solution-processed graphene oxide electrode for supercapacitors fabricated using low temperature thermal reduction". In: *RSC Adv.* 10 (37 2020), pp. 22102–22111. DOI: 10.1039/D0RA03985C. URL: http://dx.doi.org/10.1039/D0RA03985C (cit. on p. 8).

[36] D. W. Kim et al. "Highly Permeable Skin Patch with Conductive Hierarchical Architectures Inspired by Amphibians and Octopi for Omnidirectionally Enhanced Wet Adhesion". In: *Advanced Functional Materials* 29.13 (2019), p. 1807614. DOI: https://doi.org/10.1002/adfm.201807614. eprint: https://onlinelibrary.wiley.com/doi/pdf/10.1002/adfm.201807614. URL: https://onlinelibrary.wiley.com/doi/abs/10.1002/adfm.201807614 (cit. on pp. 11, 12).

[37] T. Kleiber, L. Kunz, and C. Disselhorst-Klug. "Muscular coordination of biceps brachii and brachioradialis in elbow flexion with respect to hand position". In: *Frontiers in Physiology* 6 (2015). ISSN: 1664-042X. DOI: 10.3389/fphys.2015.00215. URL: https://www.frontiersin.org/journals/physiology/articles/10.3389/fphys.2015.00215 (cit. on p. 5).

[38] E. Lam et al. "Exploring Textile-Based Electrode Materials for Electromyography Smart Garments". In: *Journal of Rehabilitation and Assistive Technologies Engineering* 9 (2022-02), p. 20556683211061995. DOI: 10.1177/20556683211061995 (cit. on p. 8).

[39] R. Lamptey et al. "A Review of the Common Neurodegenerative Disorders: Current Therapeutic Approaches and the Potential Role of Nanotherapeutics". In: *International Journal of Molecular Sciences* 23.3 (2022), p. 1851. DOI: 10.3390/ijms23031851. URL: https://doi.org/10.3390/ijms23031851 (cit. on p. 4).

[40] Y. S. Lee et al. "Softened double-layer octopus-like adhesive with high adaptability for enhanced dynamic dry and wet adhesion". In: *Chemical Engineering Journal* 468 (2023), p. 143792. ISSN: 1385-8947. DOI: https://doi.org/10.1016/j.cej.2023.143792. URL: https://www.sciencedirect.com/science/article/pii/S1385894723025238 (cit. on p. 11).

[41] J. Lévesque et al. *3D-Printed Conductive Thermoplastic Electromyography Electrodes*. 2024-05. DOI: 10.36227/techrxiv.171561021.16277667/v1 (cit. on pp. 10–12).

[42] Y. Li et al. "Flexible TPU strain sensors with tunable sensitivity and stretchability by coupling AgNWs with rGO". In: *J. Mater. Chem. C* 8 (12 2020), pp. 4040–4048. DOI: 10.1039/D0TC00029A. URL: http://dx.doi.org/10.1039/D0TC00029A (cit. on p. 11).

[43] G. Liao et al. "Using low-temperature carbon electrode for preparing hole-conductor-free perovskite heterojunction solar cells under high relative humidity". In: *Nanoscale* 8 (2015-12). DOI: 10.1039/C5NR07091K (cit. on p. 29).

[44] B. R. Liyarita, A. Ambrosi, and M. Pumera. "3D-printed Electrodes for Sensing of Biologically Active Molecules". In: *Electroanalysis* 30.7 (2018), pp. 1319–1326. DOI: https://doi.org/10.1002/elan.201700828. eprint: https://analyticalsciencejournals.onlinelibrary.wiley.com/doi/pdf/10.1002/elan.201700828. URL: https://analyticalsciencejournals.onlinelibrary.wiley.com/doi/abs/10.1002/elan.201700828 (cit. on p. 7).

[45] J. M. Lourenço. *The NOVAthesis LaTeX Template User's Manual*. NOVA University Lisbon. 2021. URL: https://github.com/joaomlourenco/novathesis/raw/main/template.pdf (cit. on p. i).

[46] L. Madanat et al. "Impact of Defibrillator Electrode Placement on Outcome of Electrical Cardioversion of Atrial Fibrillation: A Pilot Observational Study". In: *Journal of the American Heart Association* 13.13 (2024), e034817. DOI: 10.1161/JAHA.123.034817. eprint: https://www.ahajournals.org/doi/pdf/10.1161/JAHA.123.034817. URL: https://www.ahajournals.org/doi/abs/10.1161/JAHA.123.034817 (cit. on p. 1).

[47] S. K. Mangla et al. "Optimizing fused deposition modelling parameters based on the design for additive manufacturing to enhance product sustainability". In: *Computers in Industry* 145 (2023), p. 103833. ISSN: 0166-3615. DOI: https://doi.org/10.1016/j.compind.2022.103833. URL: https://www.sciencedirect.com/science/article/pii/S0166361522002299 (cit. on p. 14).

[48] G. Marco, B. Alberto, and V. Taian. "Surface EMG and muscle fatigue: multi-channel approaches to the study of myoelectric manifestations of muscle fatigue". In: *Physiological Measurement* 38.5 (2017-03), R27. DOI: 10.1088/1361-6579/aa60b9. URL: https://dx.doi.org/10.1088/1361-6579/aa60b9 (cit. on p. 33).

[49] I. Martin et al. "Advanced Thermoplastic Composite Manufacturing by In-Situ Consolidation: A Review". In: *Journal of Composites Science* 4.4 (2020). ISSN: 2504-477X. URL: https://www.mdpi.com/2504-477X/4/4/149 (cit. on p. 1).

[50] C. McCuller, R. Jessu, and A. L. Callahan. "Physiology, Skeletal Muscle". In: [Updated 2023 Jul 30]. In: StatPearls [Internet]. Treasure Island (FL): StatPearls Publishing. 2024 (cit. on p. 5).

[51] E. M. McNally and P. Pytel. "Muscle Diseases: The Muscular Dystrophies". In: *Annual Review of Pathology: Mechanisms of Disease* 2.Volume 2, 2007 (2007), pp. 87–109. ISSN: 1553-4014. DOI: https://doi.org/10.1146/annurev.pathol.2.010506.091936. URL: https://www.annualreviews.org/content/journals/10.1146/annurev.pathol.2.010506.091936 (cit. on p. 4).

[52] F. Meng et al. "Tree frog adhesion biomimetics: opportunities for the development of new, smart adhesives that adhere under wet conditions". In: *Philosophical Transactions of the Royal Society A: Mathematical, Physical and Engineering Sciences* 377.2150 (2019), p. 20190131. DOI: 10.1098/rsta.2019.0131. eprint: https://royalsocietypublishing.org/doi/pdf/10.1098/rsta.2019.0131. URL: https://royalsocietypublishing.org/doi/abs/10.1098/rsta.2019.0131 (cit. on p. 19).

[53] F. M. Mwema and E. T. Akinlabi. "Basics of Fused Deposition Modelling (FDM)". In: *Fused Deposition Modeling: Strategies for Quality Enhancement*. Cham: Springer International Publishing, 2020, pp. 1–15. ISBN: 978-3-030-48259-6. DOI: 10.1007/978-3-030-48259-6_1. URL: https://doi.org/10.1007/978-3-030-48259-6_1 (cit. on pp. 13, 14).

[54] M. Naftaly et al. "Sheet Resistance Measurements of Conductive Thin Films: A Comparison of Techniques". In: *Electronics* 10 (2021-04), p. 960. DOI: 10.3390/electronics10080960 (cit. on p. 25).

[55] D. Nam et al. "Next-Generation Wearable Biosensors Developed with Flexible Bio-Chips". In: *Micromachines* 12.1 (2021-01), p. 64. DOI: 10.3390/mi12010064 (cit. on pp. 5, 6).

[56] R. A. Nawrocki et al. "Self-Adhesive and Ultra-Conformable, Sub-300 nm Dry Thin-Film Electrodes for Surface Monitoring of Biopotentials". In: *Advanced Functional Materials* 28.36 (2018), p. 1803279. DOI: https://doi.org/10.1002/adfm.201803279. eprint: https://onlinelibrary.wiley.com/doi/pdf/10.1002/adfm.201803279. URL: https://onlinelibrary.wiley.com/doi/abs/10.1002/adfm.201803279 (cit. on pp. 11, 12).

[57] N. Ogihara et al. "Impedance Spectroscopy Characterization of Porous Electrodes under Different Electrode Thickness Using a Symmetric Cell for High-Performance Lithium-Ion Batteries". In: *The Journal of Physical Chemistry C* 119.9 (2015), pp. 4612–4619. DOI: 10.1021/jp512564f. eprint: https://doi.org/10.1021/jp512564f. URL: https://doi.org/10.1021/jp512564f (cit. on p. 30).

[58] A. Phinyomark, E. Campbell, and E. Scheme. "Surface Electromyography (EMG) Signal Processing, Classification, and Practical Considerations". In: *Biomedical Signal Processing: Advances in Theory, Algorithms and Applications*. Ed. by G. Naik. Singapore: Springer Singapore, 2020, pp. 3–29 (cit. on p. 5).

[59] T. Pinheiro et al. "Laser-Induced Graphene on Paper toward Efficient Fabrication of Flexible, Planar Electrodes for Electrochemical Sensing". In: *Advanced Materials Interfaces* 8.22 (2021), p. 2101502. DOI: https://doi.org/10.1002/admi.202101502. eprint: https://onlinelibrary.wiley.com/doi/pdf/10.1002/admi.202101502. URL: https://onlinelibrary.wiley.com/doi/abs/10.1002/admi.202101502 (cit. on pp. 7, 9, 21).

[60] T. Pinheiro et al. "Water Peel-Off Transfer of Electronically Enhanced, Paper-Based Laser-Induced Graphene for Wearable Electronics". In: *ACS Nano* 16.12 (2022). PMID: 36383513, pp. 20633–20646. DOI: 10.1021/acsnano.2c07596. eprint: https://doi.org/10.1021/acsnano.2c07596. URL: https://doi.org/10.1021/acsnano.2c07596 (cit. on p. 7).

[61] T. Pinheiro et al. "Water Peel-Off Transfer of Electronically Enhanced, Paper-Based Laser-Induced Graphene for Wearable Electronics". In: *ACS Nano* 16.12 (2022). PMID: 36383513, pp. 20633–20646. DOI: 10.1021/acsnano.2c07596. eprint: https://doi.org/10.1021/acsnano.2c07596. URL: https://doi.org/10.1021/acsnano.2c07596 (cit. on p. 21).

[62] N. Rafie, A. H. Kashou, and P. A. Noseworthy. "ECG Interpretation: Clinical Relevance, Challenges, and Advances". In: *Hearts* 2.4 (2021), pp. 505–513. ISSN: 2673-3846. DOI: 10.3390/hearts2040039. URL: https://www.mdpi.com/2673-3846/2/4/39 (cit. on p. 6).

[63] X. Ruan et al. "Emerging Applications of Additive Manufacturing in Biosensors and Bioanalytical Devices". In: *Advanced Materials Technologies* 5.7 (2020), p. 2000171. DOI: https://doi.org/10.1002/admt.202000171. eprint: https://onlinelibrary.wiley.com/doi/pdf/10.1002/admt.202000171. URL: https://onlinelibrary.wiley.com/doi/abs/10.1002/admt.202000171 (cit. on p. 8).

[64] M. Salmi. "Additive Manufacturing Processes in Medical Applications". In: *Materials* 14.1 (2021). ISSN: 1996-1944. URL: https://www.mdpi.com/1996-1944/14/1/191 (cit. on p. 1).

[65] L. Sandanamsamy et al. "A comprehensive review on fused deposition modelling of polylactic acid". In: *Progress in Additive Manufacturing* 8.5 (2023), pp. 775–799. DOI: 10.1007/s40964-022-00356-w. URL: https://doi.org/10.1007/s40964-022-00356-w (cit. on p. 14).

[66] N. Sengar, M. K. Dutta, and C. M. Travieso. "Identification of amyotrophic lateral sclerosis using EMG signals". In: *2017 4th IEEE Uttar Pradesh Section International Conference on Electrical, Computer and Electronics (UPCON)*. 2017, pp. 468–471. DOI: 10.1109/UPCON.2017.8251093 (cit. on p. 4).

[67] S. Sharma et al. "A review on electrochemical detection of serotonin based on surface modified electrodes". In: *Biosensors and Bioelectronics* 107 (2018), pp. 76–93. ISSN: 0956-5663. DOI: https://doi.org/10.1016/j.bios.2018.02.013. URL: https://www.sciencedirect.com/science/article/pii/S0956566318301015 (cit. on p. 8).

[68] A. V. Shokurov and C. Menon. "Laser-Induced Graphene Electrodes for Electrochemistry Education and Research". In: *Journal of Chemical Education* 100.6 (2023), pp. 2411–2417. DOI: 10.1021/acs.jchemed.2c01237. eprint: https://doi.org/10.1021/acs.jchemed.2c01237. URL: https://doi.org/10.1021/acs.jchemed.2c01237 (cit. on p. 1).

[69] S. L. Silvestre et al. "Cork derived laser-induced graphene for sustainable green electronics". In: *Flexible and Printed Electronics* 7.3 (2022-09), p. 035021. DOI: 10.1088/2058-8585/ac8e7b. URL: https://dx.doi.org/10.1088/2058-8585/ac8e7b (cit. on p. 7).

[70] D. A. Smith. *The sliding-filament theory of muscle contraction*. Springer, 2018 (cit. on p. 5).

[71] M. Sonoo et al. "Utility of trapezius EMG for diagnosis of amyotrophic lateral sclerosis". In: *Muscle & Nerve* 39.1 (2009), pp. 63–70. DOI: https://doi.org/10.1002/mus.21196. eprint: https://onlinelibrary.wiley.com/doi/pdf/10.1002/mus.21196. URL: https://onlinelibrary.wiley.com/doi/abs/10.1002/mus.21196 (cit. on p. 4).

[72] H. Suzuki et al. "Problems associated with the thin-film Ag/AgCl reference electrode and a novel structure with improved durability". In: *Sensors and Actuators B: Chemical* 46.2 (1998), pp. 104–113. ISSN: 0925-4005. DOI: https://doi.org/10.1016/S0925-4005(98)00043-4. URL: https://www.sciencedirect.com/science/article/pii/S0925400598000434 (cit. on p. 7).

[73] A. Synetos and D. Tousoulis. "Chapter 3.5.2 - Invasive Imaging Techniques". In: *Coronary Artery Disease*. Ed. by D. Tousoulis. Academic Press, 2018, pp. 359–376. ISBN: 978-0-12-811908-2. DOI: https://doi.org/10.1016/B978-0-12-811908-2.00018-0. URL: https://www.sciencedirect.com/science/article/pii/B9780128119082000180 (cit. on p. 27).

[74] M. Tabebordbar, E. T. Wang, and A. J. Wagers. "Skeletal Muscle Degenerative Diseases and Strategies for Therapeutic Muscle Repair". In: *Annual Review of Pathology: Mechanisms of Disease* 8.Volume 8, 2013 (2013), pp. 441–475. ISSN: 1553-4014. DOI: https://doi.org/10.1146/annurev-pathol-011811-132450. URL: https://www.annualreviews.org/content/journals/10.1146/annurev-pathol-011811-132450 (cit. on p. 4).

[75] G. Tranter. "Protein Structure Analysis by CD, FTIR, and Raman Spectroscopies". In: *Encyclopedia of Spectroscopy and Spectrometry (Third Edition)*. Ed. by J. C. Lindon, G. E. Tranter, and D. W. Koppenaal. Third Edition. Oxford: Academic Press, 2017, pp. 740–758. ISBN: 978-0-12-803224-4. DOI: https://doi.org/10.1016/B978-0-12-409547-2.12099-2. URL: https://www.sciencedirect.com/science/article/pii/B9780124095472120992 (cit. on p. 27).

[76] H. Valkenaers et al. "A Novel Approach to Additive Manufacturing: Screw Extrusion 3D-Printing". In: 2013-01, pp. 235–238. ISBN: 978-981-07-7248-2. DOI: 10.3850/978-981-07-7247-5-359 (cit. on pp. 8, 9).

[77] S. Vyavahare et al. "Fused deposition modelling: a review". In: *Rapid Prototyping Journal* 26.1 (2020), pp. 176–201. DOI: 10.1108/RPJ-04-2019-0106. URL: https://doi.org/10.1108/RPJ-04-2019-0106 (cit. on p. 14).

[78] Z. Wan et al. "Laser induced graphene for biosensors". In: *Sustainable Materials and Technologies* 25 (2020), e00205. ISSN: 2214-9937. DOI: https://doi.org/10.1016/j.susmat.2020.e00205. URL: https://www.sciencedirect.com/science/article/pii/S2214993720304218 (cit. on p. 9).

[79] F. Wang et al. "Laser-induced graphene: preparation, functionalization and applications". In: *Materials technology* 33.5 (2018), pp. 340–356 (cit. on p. 7).

[80] R. P. van Wijk van Brievingh and A. J. C. de Reus. "Electrodes for Bioelectric Signals". In: *Biomedical Modeling and Simulation on a PC: A Workbench for Physiology and Biomedical Engineering*. Ed. by R. P. van Wijk van Brievingh and D. P. F. Möller. New York, NY: Springer New York, 1993, pp. 135–155. ISBN: 978-1-4613-9163-0. DOI: 10.1007/978-1-4613-9163-0_9. URL: https://doi.org/10.1007/978-1-4613-9163-0_9 (cit. on p. 6).

[81] G. Wolterink et al. "2017 IEEE Sensors". In: *Proceedings of the 2017 IEEE Sensors Conference*. Glasgow, UK: IEEE, 2017 (cit. on p. 10).

[82] G. Wolterink et al. "Development of Soft sEMG Sensing Structures Using 3D-Printing Technologies". In: *Sensors* 20.15 (2020). ISSN: 1424-8220. DOI: 10.3390/s20154292. URL: https://www.mdpi.com/1424-8220/20/15/4292 (cit. on pp. 10, 12).

[83] H. Wu et al. "Materials, Devices, and Systems of On-Skin Electrodes for Electrophysiological Monitoring and Human–Machine Interfaces". In: *Advanced Science* 8.2 (2021), p. 2001938. DOI: https://doi.org/10.1002/advs.202001938. eprint: https://onlinelibrary.wiley.com/doi/pdf/10.1002/advs.202001938. URL: https://onlinelibrary.wiley.com/doi/abs/10.1002/advs.202001938 (cit. on p. 7).

[84] C. Yang et al. "3D-Printed Carbon Electrodes for Neurotransmitter Detection". In: *Angewandte Chemie International Edition* 57.43 (2018), pp. 14255–14259. DOI: https://doi.org/10.1002/anie.201809992. eprint: https://onlinelibrary.wiley.com/doi/pdf/10.1002/anie.201809992. URL: https://onlinelibrary.wiley.com/doi/abs/10.1002/anie.201809992 (cit. on p. 7).

[85] G. Yang et al. "MXenes-based nanomaterials for biosensing and biomedicine". In: *Coordination Chemistry Reviews* 479 (2023), p. 215002. ISSN: 0010-8545. DOI: https://doi.org/10.1016/j.ccr.2022.215002. URL: https://www.sciencedirect.com/science/article/pii/S0010854522005975 (cit. on p. 8).

[86] S. Zhang et al. "Analysis on variable stiffness of a cable-driven parallel–series hybrid joint toward wheelchair-mounted robotic manipulator". In: *Advances in Mechanical Engineering* 11 (2019-04), p. 168781401984628. DOI: 10.1177/1687814019846289 (cit. on p. 5).

[87] M. Zhu et al. "Flexible Electrodes for In Vivo and In Vitro Electrophysiological Signal Recording". In: *Advanced Healthcare Materials* 10.17 (2021), p. 2100646. DOI: https://doi.org/10.1002/adhm.202100646. eprint: https://onlinelibrary.wiley.com/doi/pdf/10.1002/adhm.202100646. URL: https://onlinelibrary.wiley.com/doi/abs/10.1002/adhm.202100646 (cit. on p. 1).